Published in final edited form as:
Neuroimaging Clin N Am. 2011 May ; 21(2): 259–283. doi:10.1016/j.nic.2011.02.007.

MR Perfusion Imaging in Acute Ischemic Stroke

William A. Copen, MD,
Director of Advanced MR Neuroimaging, Massachusetts General Hospital Department of Radiology, Division of Neuroradiology, Instructor in Radiology, Harvard Medical School

Pamela W. Schaefer, MD, and
Associate Director of Neuroradiology, Neuroradiology Fellowship Director, Clinical Director of MRI, Massachusetts General Hospital, Associate Professor of Radiology, Harvard Medical School, Boston, MA, office: (617)-726-8787

Ona Wu, PhD
Assistant in Neuroimaging, Assistant Professor of Radiology, MGH/MIT/HMS Athinoula A. Martinos Center for Biomedical Imaging, MGH Department of Radiology

Pamela W. Schaefer: pschaefer@partners.org

Abstract

MR perfusion imaging offers the potential for measuring brain perfusion in acute stroke patients, at a time when treatment decisions based upon these measurements may affect outcomes dramatically. Rapid advancements in both acute stroke therapy and perfusion imaging techniques have resulted in continuing redefinition of the role that perfusion imaging should play in patient management. This review first discusses the basic pathophysiology of acute stroke, with specific attention to alterations in the various perfusion-related parameters that can be studied by MR perfusion imaging. Although these parameters are sometimes treated as somewhat interchangeable, they reveal greatly different information about brain perfusion. Therefore, subsequent discussion of the utility of different kinds of perfusion images focuses on the differences between them, as well as important artifacts that can complicate their interpretation. Finally, research on the continually evolving role of MR perfusion imaging in acute stroke care is summarized.

Introduction

When MRI-based techniques for studying brain perfusion were developed in the 1980s and 1990s, [1] one of the first pathologic conditions to which they were applied was ischemic stroke, a disease that is caused fundamentally by impaired perfusion. Like the PET- and SPECT-based methods that preceded it, MR perfusion imaging of acute stroke patients

Corresponding author for proof and reprints: William A. Copen, MD, Massachusetts General Hospital, Neuroradiology GRB-273A, 55 Fruit Street, Boston, MA 02114, wcopen@partners.org, +1 (617) 726-8320, +1 (617) 724-3338 (fax).
Coauthors' addresses: Pamela W. Schaefer, MD, Massachusetts General Hospital, Neuroradiology GRB-273A, 55 Fruit Street, Boston, MA 02114, pschaefer@partners.org, +1 (617) 726-8320, +1 (617) 724-3338 (fax)
Ona Wu, PhD, MGH/MIT/HMS Athinoula A. Martinos Center for Biomedical Imaging, 149 Thirteenth Street Suite 2301, Charlestown, MA 02129, ona@nmr.mgh.harvard.edu, +1 617 643-2539, +1 617 726-4400 (fax)

Drs. Copen and Schaefer have no disclosures. Ona Wu has a patent on "Delay-compensated calculation of tissue blood flow," US Patent 7,512,435. March 31, 2009, and the patent has been licensed to General Electric, Siemens, and Olea Medical.

offered a window into a rapidly evolving disease process, in which changes in tissue perfusion may have dramatic effects upon patient outcomes. MR-based perfusion-weighted imaging allowed perfusion measurements to be obtained more quickly than with PET or SPECT, and with scanners that were more widely available.

Interest in imaging perfusion rapidly was spurred by the U.S. Food and Drug Administration's 1996 approval of intravenous tissue plasminogen activator (tPA), a thrombolytic drug whose purpose is restore brain perfusion, but which was approved for use only in those very few acute stroke patients who can be treated within three hours of symptom onset. Because tPA offers both the potential for lifesaving rescue of underperfused tissue and the risk of catastrophic intracranial hemorrhage, the most active focus of research on MR perfusion imaging in acute stroke has been its potential application in refining the selection of patients for thrombolysis. However, perfusion imaging also has other potential roles in ischemic cerebrovascular disease, including establishing diagnosis, predicting prognosis, and guiding non-thrombolytic therapies designed to maintain cerebral perfusion.

Before addressing MR perfusion imaging's potential uses in these roles, this review will first discuss the ways in which the various perfusion parameters that can be measured by perfusion imaging vary under different hemodynamic conditions. The following section will present the computational techniques that are used to create the various kinds of clinically used MR perfusion images. Although the details of these techniques and the artifacts that they may create are often overlooked in discussions of perfusion imaging, understanding them is essential to integrating the results of past research on MR perfusion imaging, and to utilizing perfusion imaging in patient care.

The hemodynamics of ischemic stroke

The changes in perfusion that occur in acute stroke are driven fundamentally by global and/or regional changes in cerebral perfusion pressure (CPP).[2] CPP is the difference between mean arterial pressure and venous pressure, the latter of which is usually equal to intracranial pressure. The cerebral vasculature responds to small reductions in CPP by dilating small arteries, thereby reducing cerebrovascular resistance, and successfully maintaining normal cerebral blood flow (CBF) over a wide range of perfusion pressures.[3] This vasodilatory response results in an increase in cerebral blood volume (CBV),[4] which is the volume of the intravascular space within a particular volume of brain tissue, such as that within a single image voxel. The increase in CBV may be subtle and difficult to detect in MR perfusion images. Vasodilation also results in an increase in mean transit time (MTT), which is the average amount of time that red blood cells spend within a particular volume of tissue. CBF, CBV, and MTT are related via the central volume theorem:[5]

$$MTT = \frac{CBV}{CBF}.$$

When CPP drops below the threshold at which the brain maintains autoregulation, the compensatory vasodilatory response is overwhelmed. CBF begins to fall, and becomes pressure-dependent, i.e., further reductions in CPP lead to worsening decreases in CBF. Although this reflects a decrease in the rate of oxygen delivery to the capillary bed, metabolic compromise can be avoided if CBF is only mildly reduced, because of the effect of MTT prolongation upon oxygen extraction. When MTT is increased, red blood cells spend a longer time within oxygen-permeable capillaries, and this allows for an increase in the proportion of the available oxygen that can be extracted from the blood by the brain (oxygen extraction fraction, or OEF). If the CBF reduction is mild, the increase in OEF is

sufficient to maintain oxygen metabolism (cerebral metabolic rate of oxygen consumption, $CMRO_2$), and neither the brain's electrical function nor its viability is threatened.[6] This level of hypoperfusion has been called "benign oligemia,"[7] although that term has also been used to refer less specifically to any underperfused state that does not threaten tissue viability, regardless of whether electrical function is preserved.[8]

With even further reductions in CPP, CBF falls so low that increased oxygen extraction is unable to maintain normal oxygen metabolism, and $CMRO_2$ falls. With a sufficient reduction in $CMRO_2$, neurons cease their electrical transmission, and the patient may experience a neurologic deficit. If the $CMRO_2$ reduction is mild enough, the survival of the tissue is not threatened, despite its electrical silence, and this situation can persist indefinitely without permanent damage. If there is an even more severe reduction in CPP, and therefore an even greater reduction in CBF, $CMRO_2$ falls to such a low level that the survival of the affected tissue is threatened. One of the most important principles of ischemic pathophysiology is that the time that it takes for ischemic damage to become irreversible is inversely related to the severity of the ischemia.[9] Brain tissue dies after just a few minutes without any blood flow, but moderately ischemic tissue may remain potentially viable for hours before becoming irreversibly injured. A primary goal of perfusion imaging in acute stroke is the identification of tissue that may be a target for thrombolytic therapy, in that it is threatened by ischemia, but still may be potentially salvageable. Tissue that is still structurally intact and hence viable but electrically dysfunctional has been called the "ischemic penumbra,"[10] with the word "penumbra" chosen because the mildly ischemic tissue sometimes forms a ring-like shape, surrounding a central area ("infarct core") where more severe ischemia has resulted in irreversible injury. It has been suggested that the term can be more usefully redefined to describe tissue that is potentially therapeutically treatable.[11]

It has been suggested[2] that, in conditions of extremely low CPP, low CBV may occur despite maximal vascular relaxation, perhaps because perfusion pressure is so low that the patency of blood vessels cannot be maintained. However, the early studies on which current understanding of cerebral hemodynamics is based offer little direct evidence of the occurrence of decreased CBV. These studies focused more often on the CBV/CBF ratio (i.e. MTT), rather than CBV itself.[2] When early studies did measure CBV within infarcts, they often found that CBV was elevated, although these measurements were usually made in subacute infarcts that were days to weeks in age. [12-14] One study found that, in an experimental model, macrovascular and microvascular CBV became uncoupled in response to severe hypotension, with macrovascular CBV increasing in some anatomic regions while microvascular CBV decreased.[15]

If the arterial lesion that caused ischemia resolves, either spontaneously or as a result of treatment, the affected tissue is reperfused. Reperfusion can occur in both viable and nonviable tissue, and therefore the absence of any apparent hypoperfusion does not preclude the existence of completed infarction. Reperfusion is the goal of thrombolytic therapy, and it also has been seen spontaneously within eight hours of stroke onset in 16% of patients,[16] within 48 hours of onset in 33% of patients,[17] and within one week of onset in 42% to 60% of patients.[18, 19] When reperfusion occurs, either spontaneously or as a result of therapeutic intervention, resistance vessels within the previously ischemic tissue sometimes remain inappropriately dilated for hours to days, despite reestablishment of normal CPP.[20] In this situation, CBV remains high, and CBF is elevated to above-normal levels. Various studies have reported that this state of post-ischemic hyperperfusion may occur in tissue that both has and has not undergone irreversible infarction.[21, 22] In either case, blood flow is greater than required for the tissue's metabolic needs, a situation that has been called "luxury perfusion."[23]

Table 1 lists the effects of different hemodynamic conditions upon the three physiologic parameters that are most often measured with perfusion imaging: CBV, CBF, and MTT. Table 1 also includes the changes that are most often seen in various non-physiologic "timing parameters" that can be measured with perfusion imaging. In acute stroke, perfusion imaging is capable of defining perfusion conditions in different parts of the brain as apparently normal, or assigning them to one of the four abnormal categories listed in Table 1: delayed bolus arrival with preserved CPP, compensated low CPP, underperfused, or post-ischemic hyperperfusion. Of note, irreversibly injured tissue can exist in any of these four categories, and can also exhibit apparently normal perfusion.

Dynamic susceptibility contrast imaging: Basic physics and image acquisition

Because currently available techniques quantify the passage of blood through vessels that are too small to visualize directly with standard clinical MRI scanners, MR perfusion imaging must rely upon detection of tracer agents within blood, rather than direct visualization of the vessels. This review will focus on dynamic susceptibility contrast (DSC) imaging, the technique that is used for MR perfusion imaging of acute stroke in most clinical centers. Arterial spin labeling (ASL) [24] is another technique for measuring perfusion without requiring exogenous contrast agents that currently is rarely used in acute stroke imaging, because of its low signal-to-noise ratio, relatively long imaging times, and its difficulty in distinguishing between reduced blood flow and delayed transit times. Ongoing research seeks to eliminate artifacts, and ASL offers great potential for the future.

DSC uses a gadolinium chelate as an exogenous contrast agent. Although conventional contrast-enhanced MRI relies on the T1 effects of gadolinium to detect increased permeability of the blood brain barrier, in DSC, image contrast is based instead on gadolinium's susceptibility effect.[25] This is done because the T1 relaxivity effect of gadolinium extends over extremely short distances. If the blood brain barrier is intact, as is usually the case in acute stroke, only the approximately 1% to 7% of water spins that are also within blood vessels [26] would experience an appreciable change in T1 relaxation, and the pulse sequence's ability to detect small changes in local concentrations of gadolinium would be limited. However, the susceptibility effect of gadolinium ions inside of blood vessels extends over a range that is comparable in magnitude to the radius of the blood vessel, which is many orders of magnitude larger than gadolinium's T1 effects. Therefore, all water spins within a voxel may be affected by the presence of the gadolinium, and the resulting signal change is much larger than the signal change that would have been caused by T1 effects.

In DSC, susceptibility-sensitive images are acquired dynamically during the passage of a gadolinium-based contrast agent (CA) through the brain. As the CA arrives in the brain and then washes out again, first the large arteries demonstrate a transient loss in signal intensity, followed by transient parenchymal signal loss as the CA moves through smaller vessels, and then finally signal loss in the large intracranial veins (Figure 1). In order to create high-quality perfusion maps, the passage of CA in each part of the brain must be measured with high temporal resolution. Ideally, images should be obtained no less frequently than one every 1.5 seconds for human stroke imaging, assuming a normal mean transit time of approximately 3 to 4 seconds.[27] This is generally accomplished using an echo planar imaging (EPI) pulse sequence, which permits acquisition of an entire image slice with only a single radiofrequency excitation. Either spin-echo (SE) or gradient-echo (GRE) EPI images can be used. However, because SE EPI images are less sensitive to gadolinium's susceptibility effects, using a SE EPI pulse sequence at 1.5 Tesla requires injecting a larger dose of the contrast agent, typically 0.2 mmol/kg, while a standard dose of 0.1 mmol/kg is

usually sufficient for GRE EPI imaging. However, because susceptibility effects are more pronounced at higher field strengths, the standard dose of 0.1 mmol/kg may be sufficient for SE EPI perfusion imaging at field strengths of 3 Tesla or higher. Nevertheless, GRE imaging is performed more often than SE imaging at all field strengths. The pulse sequence parameters used at the authors' institution are listed in Table 2. All of the examples depicted in this review were generated using these parameters.

The physical basis of image contrast in DSC results in several noteworthy properties of the perfusion maps that DSC produces. First, DSC's sensitivity to changes in precession frequency of all of the spins within each brain voxel gives the technique far greater sensitivity for detecting changes in contrast agent concentration than CT perfusion imaging, which relies on the x-ray attenuation of an iodine-based contrast agent that remains within the intravascular space (Figure 2). CT perfusion post-processing algorithms usually compensate for the far greater noise level within their source images by performing spatial and temporal blurring, which is not usually done in DSC post-processing. Second, unlike CT perfusion imaging, which is equally sensitive to the presence of the contrast agent within vessels of all sizes, DSC produces different degrees of signal change for similar quantities of gadolinium in blood vessels of different sizes.[28] GRE EPI is more sensitive to CA in larger vessels, whereas SE EPI demonstrates greater sensitivity to CA in smaller vessels. Some DSC pulse sequences exploit this vessel-size sensitivity by acquiring both SE and GRE images during the same contrast injection, enabling elementary measurements of the relative proportions of smaller and larger blood vessels. Although this interleaved technique has shown promise in assessing neovascularity within brain tumors, [29] it is not generally used in acute stroke imaging. However, findings in animal models suggest that combining GRE- and SE-based perfusion imaging may provide improved insight into tissue status after stroke.[15]

Dynamic susceptibility contrast imaging: Measurement of perfusion parameters

Overview

Direct inspection of DSC images can yield rudimentary information about regional brain perfusion, and this approach is sometimes useful when severe patient motion precludes additional postprocessing. However, under most circumstances, individual DSC images like those in Figure 1 undergo additional post-processing to produce maps of various perfusion-related parameters, in which each pixel's value reflects a single scalar measurement that is derived from the signal intensity-versus-time function for the corresponding voxel. It is these maps that are interpreted in the clinical setting. Many different perfusion measurements can be derived from DSC images, but five are most commonly used: time to peak contrast concentration (TTP), cerebral blood volume (CBV), cerebral blood flow (CBF), mean transit time (MTT), and time at which the deconvolved residue function reaches its maximum value (Tmax).

Examples of these five perfusion maps, illustrating each of the four abnormal perfusion conditions listed in Table 1, are presented in Figures 3 through 6. As is evident from these examples, the various kinds of perfusion maps vary greatly in appearance, and they provide vastly different information about brain perfusion.[30] Nevertheless, it has become commonplace for published stroke imaging papers to refer to these maps generically as "perfusion imaging," and this has led to considerable confusion and inconsistency. Confusion surrounding the different types of perfusion maps is exacerbated by the fact that, although most of these perfusion maps (specifically CBV, CBF, and MTT) ostensibly depict well-defined fundamental physiologic parameters, detailed examination of the algorithms

that are used to compute them reveals a number of major technique-dependent artifacts. In order to best understand the use of perfusion imaging in the care of stroke patients, it is important to understand in some detail the post-processing techniques that are used to create each kind of perfusion map, and the artifacts that they may introduce.

Time to peak concentration (TTP)

Of the five parameters that will be discussed here, TTP is the simplest to calculate, and provides the least specific information about brain perfusion. In each voxel, TTP is the time at which signal intensity reaches its minimum, and therefore contrast concentration reaches its maximum. For example, for a particular DSC acquisition in which images are acquired every 1.5 seconds, possible TTP values could include 20.0 seconds, 21.5 seconds, 23.0 seconds, etc.

Numerous studies have used increases in regional TTP for putative identification of brain tissue that is threatened by ischemia,[31–38] including one clinical trial that used DWI-TTP mismatch to select patients for intravenous thrombolytic therapy outside of the usual three-hour time window.[39] The advantages of TTP in this role are that lesions in TTP maps are conspicuous and usually well-defined, and that TTP is a reproducible technique, in that measurements obtained by different centers from a single data set are similar, with less technique-dependent artifacts to complicate interpretation. TTP is very sensitive to motion artifacts and noise so some algorithms that perform motion correction and pre-filtering will produce differing results. Some algorithms also perform curve fitting to obtain TTP. A primary disadvantage of using TTP is that TTP can be prolonged in a wide variety of acute and chronic hemodynamic conditions, in which tissue viability may or may not be threatened. As shown in Figures 3 through 5, and 7, TTP prolongation may be caused by reduced blood flow, but also occurs when the arrival of the injected contrast bolus is delayed, but CBF is normal. In some circumstances, TTP may even be prolonged in reperfused tissue whose CBF is higher than normal, tissue whose survival clearly is no longer threatened by ischemia.

Converting signal changes to concentration measurements

Calculation of all of the four remaining perfusion parameters that will be discussed here relies on a common first step: conversion of each voxel's signal intensity-versus-time curve into a CA concentration-versus-time curve. In order to accomplish this conversion, the signal intensity-versus-time curve must be divided into two portions, reflecting signal intensity prior to and after arrival of the injected contrast bolus, respectively. Prior to bolus arrival, signal intensity fluctuates slightly, due to random noise, around a baseline value that is determined by time-invariant properties of the tissue within the voxel and the pulse sequence that is used. Pre-injection points are typically averaged to produce an estimate of baseline signal intensity, S_0. Following the arrival of the bolus, the concentration of gadolinium in a voxel can be derived from signal intensity by the equation

$$C(t) = -k \ln\left(\frac{S_t}{S_0}\right),$$

in which C(t) is the CA concentration at a particular time *t*, S_t is the signal intensity at that time, S_0 is the baseline signal intensity before the arrival of the contrast agent, and *k* is a constant whose value depends upon the pulse sequence used, the manner in which the contrast is injected, and complex characteristics of the patient's circulatory system that are difficult to model. [28] Because the value of *k* is difficult to estimate, absolute perfusion

measurements are difficult to obtain, and most perfusion maps provide only relative quantification of perfusion parameters. Although techniques have been proposed for computing absolute measurements of CBF with MR perfusion imaging, these measurements, like those obtained from CT perfusion imaging, typically vary by as much as a factor of two or three, compared to those obtained by gold-standard methods such as xenon CT and positron emission tomography (PET).[40–51]

Cerebral Blood Volume (CBV)

Of the remaining four perfusion parameters (CBV, CBF, MTT and Tmax), calculation of CBV is the simplest, requiring the fewest additional computational steps. Although CBV was one of the first perfusion parameters to be derived from MR perfusion imaging in human stroke,[52] MR CBV maps historically have had little utility in acute stroke imaging, because the role that was presumptively assigned to them is better filled by DWI. The lesion seen on DWI is generally accepted to be the best available indicator of the irreversibly injured tissue in the infarct core. Several studies found that, CBV maps often demonstrated a low-CBV lesion whose volume was small, like that of the DWI lesion, and that the volumes of both lesions served well as a lower limit of the volume of the infarct that was ultimately seen in later follow-up images. [53–57] Because of these observations, it was suggested that CBV maps, like DWI, could be used to identify the infarct core. However, CBV maps were rarely used for this purpose in practice, because lesions in DWI images are far more conspicuous and clearly delineated than those in CBV maps. In addition, many of these studies used SE-EPI for the data acquisition, which is more sensitive to smaller vessels that may experience injuries earlier than larger vessels, while currently the majority of clinical MRI centers use GRE-EPI.

Interest in using CBV maps to define the infarct core increased greatly with the emergence of CT perfusion imaging. Although CT- and MR-based techniques can provide similar perfusion maps, there is no CT equivalent for DWI, and so there is no accepted way to identify the infarct core without MRI. Some authors have suggested that the core can be identified by CT-derived CBV maps, thereby obviating the need for DWI.[58] This practice implicitly accepts that the significant proportion of core tissue that experiences spontaneous reperfusion will not be identifiable as such, and that the diagnosis of stroke may be missed if the entire infarct has reperfused.[59] Even without reperfusion, the notion that CBV is reduced in the infarct core contradicts the physiologic principle that blood vessels dilate in underperfused tissue, in order to recruit additional blood flow. Although it has been hypothesized that CBV may drop when extremely low perfusion pressures cause vascular collapse, this phenomenon is poorly documented, and its prevalence is unclear.

The apparent contradiction between MR- and CT-based findings of reduced CBV in the infarct core, and theoretical and empirical predictions of elevated CBV, may be explained by artifactual flow- and delay-weighting that are introduced by the algorithms that are used to calculate CBV. CBV theoretically could be calculated by integrating the area under the CA concentration-versus-time curve, $C(t)$, for the first pass of the injected contrast bolus through each voxel. However, measuring just the first pass is difficult, because recirculation usually results in the arrival of the second pass before the first pass is complete, and the two passes therefore are summed together in the measured $C(t)$. Some researchers have attempted to extract the first pass of the contrast bolus by fitting gamma variates[60] or other functions[61] to the first portion of $C(t)$. However, no particular model has been shown to reflect the first pass reliably.

Because of these challenges, CBV is usually calculated by numerically integrating the area under the entire $C(t)$. This method produces truly accurate CBV measurements only for infinitely long scan durations, because, as the time post-injection approaches infinity, CA

concentration in all parts of the brain approaches steady state. However, actual MR perfusion perfusion scans have finite durations, typically on the order of 60 seconds. During that time, the CA concentration-versus-time curves in different parts of the brain may reflect different numbers of passes of the contrast agent. Specifically, in regions where the arrival of the contrast bolus is delayed, and/or low regional CBF results in a slower rate of arrival of the contrast bolus, *C(t)* is effectively truncated. Fewer passes of the contrast bolus will be recorded in a particular finite time period, and CBV will be underestimated, in comparison to other parts of the brain. In effect, CBV maps produced by this method are flow-weighted and delay-weighted.

Unfortunately, bolus arrival delay and decreased blood flow are common phenomena in acute stroke. When an injected CA bolus reaches brain tissue via a pathologically narrowed artery, or via long collateral perfusion pathways, its arrival is delayed, and CBV is therefore underestimated. If the arterial lesion is severe enough to cause a CBF reduction, this too will cause underestimation of CBV. This artifact is mitigated by longer scan durations, and is exacerbated by shorter scan durations (Figure 8). Some centers have employed scans as short as 40 seconds, which usually is not long enough even to completely sample the first pass of the bolus in tissue with low CBF.

Truncation of *C(t)* by short scan durations can produce artifactually large low-CBV lesions (Figure 9), and may produce apparent low-CBV lesions where low CBV doesn't actually exist (Figure 10). One recent study[62] found that, within DWI-delineated infarct cores, calculated CBV increased with increasing duration of the perfusion scan. When the longest scan duration of 110 seconds following contrast injection was used, the majority of infarcts demonstrated above-normal CBV. This study demonstrated that CBV measurements are technique-dependent, producing lesions whose presence and size are dependent upon scan duration and post-processing algorithms. When low CBV is truly present, this is likely to reflect microvascular collapse that is indicative of ischemia so severe that tissue viability is unlikely. However, it appears that many apparent low-CBV lesions in acute stroke may be artifactual, so that CBV cannot substitute for DWI in identifying the infarct core.

Cerebral Blood Flow (CBF)

Of the major parameters derived from MR perfusion images, CBF is the most directly connected to tissue viability, because CBF measures the rate of delivery of oxygen and glucose to ischemic brain tissue. Seminal animal experiments demonstrated that CBF thresholds for tissue viability exist, with threatened tissue surviving for longer periods of time when CBF is more mildly reduced. [9] Furthermore, from a qualitative perspective, examination of Table 1 shows that, of the major perfusion parameters, CBF is the only one that can reliably identify underperfused brain tissue, and distinguish it from tissue with normal or elevated blood flow. Nevertheless, CBF maps are seldom used to identify threatened brain tissue, and no major clinical trial to date has used CBF maps to select patients for experimental thrombolytic therapy.

The preference for using the less physiologically relevant TTP, MTT, and Tmax maps may be due to greater lesion conspicuity on these maps, compared to CBF maps. Like CBV maps, CBF maps demonstrate considerable heterogeneity in normal tissue, because CBV and CBF values are several times greater in gray matter than in white matter. [26] Consequently, it can be difficult to distinguish underperfused gray matter from normally perfused white matter. Lesions may also be difficult to detect in CBF and CBV maps because brain parenchyma must be distinguished from large blood vessels, which "bloom" in GRE perfusion maps, and appear larger than they actually are. In contrast, when TTP, MTT, and Tmax maps are used, gray matter-white matter differences are greatly reduced,

and macroscopic blood vessels are reduced in conspicuity, resulting in lesions that are easier to detect and delineate.

Calculation of CBF is more complex than calculation of TTP and CBV. Roughly speaking, CBF in any voxel is related to the slope of increase of *C(t)* as the CA bolus arrives. Indeed, if images are acquired with greater temporal resolution than is currently feasible in most clinical settings, CBF can be calculated by measuring this slope.[63] However, in current practice, quantitative computation of CBF requires incorporation of the concentration-versus-time curve not just in the voxel, but also in the arteries that supply blood to that voxel. In an idealized experiment, the contrast agent would be injected directly into a small artery supplying a tissue voxel, such that the concentration of CA in the artery is a unit value for a single instant in time, and zero otherwise. If this could be achieved, then the observed *C(t)* in the voxel would be a so-called "residue function" that reaches its maximum instantly, and decays gradually, reflecting the proportion of the CA remaining in the vessel over time.

However, in reality, the contrast agent is injected over several seconds, into a peripheral vein. The injected bolus must then pass through systemic veins, the heart, the pulmonary circulation, and systemic arteries before it arrives in the brain.[64, 65] In the process, the duration of the bolus is further increased, and its *C(t)* profile is reshaped in complex ways that are difficult to model. This bolus reshaping changes the concentration-versus-time function in the voxel, which is observable, but it does not change the residue function, which cannot be observed directly. Mathematically, the observed *C(t)* is the *convolution* of the arterial input function (AIF), which describes the CA concentration versus time in the artery supplying the voxel, and a multiple of the residue function in the voxel that has been scaled by the value of CBF (Figure 11).

In order to compute CBF, an AIF is calculated by measuring *C(t)* in voxels near an artery or arteries, and averaging those *C(t)* functions. This process may be accomplished manually, or automatically. [45, 66–68] After an AIF has been generated, *deconvolution* can be used to derive the scaled residue function in each voxel from the AIF and the voxel's *C(t)* function. The amplitude of the deconvolved signal is measured as the CBF, and the time at which this maximum value is reached, is called Tmax (see below). From this description, it is apparent that a single MR perfusion data set could be processed by different centers to yield different CBF maps, depending on two factors: the deconvolution algorithm that is used, and the AIF that is chosen. The deconvolution algorithm generally used for MR perfusion imaging is singular value decomposition (SVD), an algorithm that is model-independent, in that it makes no assumptions regarding the shape of the AIF, residue function, or voxel concentration function.[69–71]

If scan duration is very short, and/or bolus arrival is highly delayed, the passage of the bolus may be inadequately sampled, and calculated CBF values will be artifactually low. Artifactual underestimation of CBF with short scan durations is less severe than underestimation of CBV, and occurs only at very short scan durations (Figure 11). However, the versions of the SVD algorithm that were used in the great majority of published research on stroke suffer from a different artifact: they artifactually underestimate CBF in regions where the arrival of the contrast bolus is delayed, relative to its arrival in the AIF. [72–74] One simulation found that bolus arrival delays of 1.5–2.0 seconds may result in underestimation of CBF by approximately 35%, with even greater underestimation also possible due to bolus dispersion.[72] Unfortunately, delays of at least this magnitude are typical in tissue that is supplied by stenotic arteries. Therefore, such tissue will appear underperfused in CBF maps, even if CBF is actually preserved at a normal level by vasodilation and/or collateral circulation.

Several methods have been employed to overcome the delay artifact. One approach is to define the AIF by sampling arteries that are as close as possible to the infarct, distal to any proximal arterial lesions, in order to minimize delay between bolus arrival in the AIF and arrival in the tissue of interest.[75] A second approach is to use numerous "local AIFs" instead of a single global AIF. In the local AIF approach, the AIF for each voxel is constructed by searching in its immediate vicinity for other voxels whose concentration-versus-time curves seem most artery-like. [76–7879, 80] In theory, these local AIFs better approximate not only bolus arrival times, but the varying shapes of the actual AIFs in each voxel. However, in practice, most voxels do not have a macroscopic artery that can be sampled within their immediate vicinity, so that generating a local AIF that truly reflects arterial concentrations rather than tissue concentrations is technically complex.[81, 82] The local AIF technique is not generally used in clinical practice.

Some post-processing algorithms attempt to compensate for the arrival delay artifact by using a single global AIF, but shifting this AIF in time for each voxel, so that AIF arrival time matches the arrival of the bolus in the tissue. [83, 84] Although this approach is used by some manufacturers of CT perfusion post-processing software, in MR perfusion post-processing, it has been largely supplanted by improved versions of the SVD algorithm that do not require curve-shifting, because the techniques are insensitive to the delay artifact. One delay-insensitive SVD algorithm uses a block-circulant deconvolution matrix with oscillation index regularization.[85] This algorithm is sometimes known simply as "circular deconvolution," however, using a block-circulant matrix for deconvolution without oscillation index regularization will likely underestimate normal to high flow rates, and precise description of the technique used is important. There is increasing recognition of the potential importance of delay-compensated or delay-insensitive deconvolution in perfusion post-processing.[27]

Mean Transit Time (MTT)

MTT, like TTP, is frequently used in acute stroke imaging for putative identification of threatened brain tissue.[86–91] When MTT is used for this purpose, the region of DWI-MTT mismatch, like the region of DWI-TTP mismatch, is presumed to define tissue that is at risk. Like lesions in TTP maps, lesions in MTT maps are relatively easy to identify and delineate, because gray matter-white matter heterogeneity is minimized in MTT maps, and large vessels do not greatly impair lesion identification. MTT maps offer the advantage that they measure a parameter that is of more direct physiologic relevance, in that elevations in MTT reflect the autoregulatory response of the cerebral vasculature to a perceived drop in perfusion pressure. If a delay-insensitive deconvolution technique is used (see discussion of CBF above), MTT remains normal in regions where bolus arrival delay is delayed but perfusion is otherwise normal, and MTT is unlike TTP in this respect.

When MTT is used for identification of threatened tissue, it is sometimes stated that tissue with prolonged MTT is necessarily underperfused, and this is a misconception. Although MTT prolongation occurs in regions of vasodilation with decreased CBF, MTT is also prolonged when vasodilation results in successful preservation of normal CBF. This can be appreciated by considering Table 1, and the relationship defined by the central volume theorem, above; if CBV is elevated, but CBF is normal, then MTT, which is the quotient of CBV divided by CBF, is elevated. Tissue with elevated MTT but normal CBF may persist indefinitely in this state, without any threat to its survival, and this condition probably exists, for example, in many patients with chronic carotid stenosis. Nevertheless, although tissue metabolism remains normal if CBF is preserved, it is misleading to argue that tissue with elevated MTT but normal CBF should always be considered safe, for two reasons. First, if the vasodilation that leads to MTT elevation is caused by thromboembolic narrowing of a proximal artery, small emboli may break off of the main lesion and cause infarcts within the

region of prolonged MTT. Second, preservation of normal CBF in regions of prolonged MTT often depends upon collateral arterial supply, and collateral vessels may fail over time.

In light of these considerations, it is probably a reasonable approach to conclude that tissue with elevated MTT and reduced CBF is more severely and immediately threatened by ischemia, whereas tissue with elevated MTT but normal CBF experiences some smaller and perhaps less urgent degree of risk. Further complicating interpretation of MTT maps is the fact that MTT is sometimes prolonged in the setting of elevated CBF and elevated CBV, a condition that presumably does not pose any threat to tissue survival. In post-ischemic hyperperfusion, CBV and CBF are both elevated, and their quotient, MTT, may be either elevated or decreased, depending on which of CBV and CBF is the more elevated. Because tissue with elevated MTT may be at relatively high risk of infarction, low risk, or no risk, depending on the associated CBF value, it may be advisable to consult CBF maps when evaluating an MTT lesion.

In interpreting MTT maps, it is also worthwhile to consider how the algorithms that produce them may lead to artifacts. Post-processing software usually generates an MTT value for each voxel by first computing CBV and CBF, using the methods described above, and then dividing CBV by CBF. Most published studies in which MTT was evaluated as an indicator of tissue at risk have used delay-sensitive deconvolution to calculate CBF, which results in overestimation of MTT, and overestimation of the size of the MTT lesion. Also, shorter perfusion scans, which lead to increasing flow- and delay-weighting of CBV calculations, can lead to underestimation of MTT, and underestimation of the size of MTT lesions (Figure 10). Other studies have measured MTT using parameters derived from the shape of the *C(t)* curve, and then calculated CBF indirectly by dividing CBV by MTT.[92] Caution is therefore warranted when comparing results across studies.

Time of maximum value of the residue function (Tmax)

The third and final perfusion parameter that is derived from deconvolution is Tmax. Whereas CBF reflects the maximum value of the deconvolved residue function in each voxel, Tmax is the time at which this maximum value is reached. The value of Tmax therefore reflects bolus arrival time, with larger Tmax values reflecting later arrival of the injected contrast bolus in the voxel. Tmax is a nonphysiological paramter, in that the viability of brain tissue presumably does not depend directly upon how long it takes for blood to travel from the arm to the brain. Although high Tmax values have been correlated with lower likelihood of tissue survival,[93, 94] Tmax may be prolonged in tissue with low, normal, or high CBF, and very large volumes of tissue may exhibit prolonged Tmax without proceeding to infarction.[95] Nevertheless, Tmax has been used as a predictor of tissue viability in various studies,[93, 94, 96, 97] including two major trials testing the use of thrombolytic therapy outside of the usual three- or 4.5-hour time windows.[98, 99] Tmax has several advantages in this role. Like TTP and MTT maps, Tmax maps are relatively easy to interpret, with little gray matter-white matter heterogeneity, and relatively low conspicuity of large blood vessels that may complicate evaluation of brain parenchyma. Like TTP values, calculated Tmax values have discrete values that are equal to multiples of the TR that is used, and this often creates lesions that are easy to measure, because their boundaries are well defined. Tmax values are relatively unaffected by scan duration, provided the scan is long enough to detect the arrival of the contrast bolus in all parts of the brain (Figure 11). However, some have speculated that Tmax is a reflection of extent of collateral perfusion.[100, 101]

Using MR perfusion imaging in patient care

Diagnosis of transient ischemic attack

DWI has become the gold standard for imaging detection of acute stroke, with sensitivity and specificity approaching 100%.[34, 102–108]. DWI's unique ability to confirm or exclude the diagnosis of stroke can be of critical importance, because the etiology of stroke-like symptoms is not always initially clear.[109] Establishing the diagnosis of cerebral ischemia can be especially difficult for transient ischemic attack (TIA) patients whose symptoms have resolved before the time of presentation, and therefore cannot be evaluated by physical examination. Correct diagnosis of TIA is critical because up to 17% of TIA patients suffer a stroke within 90 days of their TIA. [110–112]. In approximately 44% of TIA patients, DWI shows an asymptomatic infarct that confirms the diagnosis.[113] Imaging of the major cervical arteries with ultrasound, or with CT or MR angiography, may also demonstrate stenosis that suggests a vascular etiology. However, many TIAs, such as those due to cardiogenic emboli, can occur in patients without significant arterial pathology. In these patients, the presence of an abnormality on perfusion imaging may be the only objective indication of ischemic etiology. In various studies, perfusion abnormalities have been found in between 3% and 25% of TIA patients who have no DWI abnormality.[114–116] It is likely that many of the patients in these studies would have been discharged home without a clear diagnosis if they had not undergone perfusion imaging, and therefore would have been deprived of a potentially lifesaving admission for workup of their TIAs.

Selection of patients for thrombolysis

The most widely available treatment for acute stroke is recombinant tissue plasminogen activator (tPA), which can improve patient outcomes by reperfusing and thereby rescuing ischemic tissue, but can also cause symptomatic intracranial hemorrhage (sICH). In order to maximize the potential for patient benefit and minimize the risk of hemorrhage, tPA's use was initially restricted to patients who could be treated within 3 hours of the time when they were last known to be without symptoms. The particular choice of three hours as the time limit for tPA administration was based on the fact that the landmark 1995 National Institute of Neurologic Disorders and Stroke (NINDS) trial[117] used a three-hour limit and showed a benefit for tPA, whereas the European Cooperative Acute Stroke Study (ECASS)[118] used a six-hour limit and was not successful. The three-hour cutoff was also supported by later thrombolysis trials that failed to show a benefit of thrombolysis when utilizing six-[119] or five-[120] hour limits, as well as a 2007 retrospective study that confirmed that thrombolysis within three hours had been safe and effective in a large cohort.[121] A further refinement was provided in 2009, when the ECASS-III study [122] achieved success using a 4.5-hour window in a carefully selected stroke population, and this longer window consequently has been adopted by many centers.

The imposition of a strict time limit on thrombolytic therapy ignores the considerable variation that exists between individual stroke patients. In the above thrombolysis trials, the only imaging study that was required was a non-contrast CT scan, a study that is highly insensitive for acute stroke. It is likely that some patients who present only one hour after symptom onset have no remaining threatened tissue that could be rescued by thrombolysis, whereas some patients scanned eight hours after onset could still benefit from treatment. Furthermore, large numbers of patients are deemed ineligible for thrombolysis because the current time limit conservatively specifies that the patient must be treated within three or 4.5 hours of the time when he or she was last known to be without symptoms, not from the time when symptoms were discovered. Numerous patients are excluded from treatment because the exact stroke onset time cannot be ascertained with certainty, either because the patient's deterioration was not witnessed, or because the patient's symptoms were first noted when he

or she awakened from sleep.[88, 123] Only 1%–7% of stroke patients receive thrombolytic therapy, [124–126] and the most common reason for ineligibility is inability to document the absence of symptoms within the required time window. [126, 127]

MR perfusion imaging, when combined with DWI, offers the potential for customized patient-specific assessments of the potential risks and benefits of thrombolysis. This could allow for widening or even abandonment[128] of the three- or 4.5-hour time window, thereby making treatment available for vastly increased numbers of patients. Indeed, the search for a role for perfusion imaging in assessing eligibility for thrombolysis has formed one of the most active areas of research in MR perfusion imaging of acute stroke patients during recent years. Broadly speaking, this research has been guided by the following hypotheses. First, in an acute stroke MRI examination, the DWI lesion reflects the irreversibly injured infarct core. Second, the likelihood of infarct growth in the days following presentation can be predicted by perfusion imaging, because infarct expansion occurs into regions of moderately impaired perfusion that lie outside of the initial DWI lesion. Third, if the preceding hypotheses are correct, then the time window for thrombolytic therapy can be widened, provided that treatment is limited to those patients who have a significant mismatch between lesions in DWI and perfusion maps.

The first hypothesis is supported by observations that initially DWI-abnormal tissue usually proceeds to infarction in follow-up images, and that the volume of the early DWI lesion usually, though not always, is smaller than that of the ultimate infarct. [31, 52, 55–57, 129, 130] Some studies have contradicted this hypothesis, by showing that reversal of DWI lesions can occur, usually in the setting of early vessel recanalization. In one such study,[96] six of seven patients demonstrated reversal of part of their DWI abnormalities following successful intra-arterial intervention with recanalization, although a subsequent increase in infarct volume was seen in three of those patients. In another study,[131] an ultimate reduction in the sizes of DWI lesions was seen in one of eleven patients whose infarcts did not recanalize, and in six of sixteen patients whose infarcts did recanalize. However, the median reduction in lesion size in this study was only 2.75 cc, and in some cases, lesion size reduction may have been due to encephalomalacic volume loss. A much larger study estimated the prevalence of DWI lesion reversal to be 0.2% to 0.4%.[132]

The second hypothesis, that perfusion imaging can be used to predict infarct growth, has received broad support from studies showing that infarct growth is more likely to occur in patients with a large mismatch between lesions seen in DWI images and those in perfusion maps, regardless of whether the perfusion parameter used is TTP, [31, 33] CBF,[130] delay-sensitive MTT, [8, 86, 133] or, in one study, a non-deconvolution-based parameter that provided an estimate of MTT.[134] These results suggest that, even if thrombolytic therapy is not under consideration, perfusion imaging may help in prognostication by suggesting the possibility of impending clinical worsening.

The final hypothesis, that the therapeutic window can be safely widened if thrombolysis is offered only to patients with a mismatch between lesions seen in DWI and perfusion maps, has been addressed by a small number of clinical trials, all but one of which were successful. The first[39] was a non-placebo-controlled trial in which patients were made eligible for tPA between three and six hours after stroke onset if they demonstrated at least a 50% DWI-TTP mismatch, as estimated by gross visual inspection at the scanner console at the time of imaging. The study's report did not specify whether DWI lesion size or TTP lesion size was used as the denominator in this calculation. Among the 43 patients who were treated in the extended time window, rates of recanalization, hemorrhagic transformation, and neurological improvement were similar to those seen in 79 patients who were treated between zero and three hours after stroke onset, using standard selection criteria.

The Desmoteplase in Acute Ischemic Stroke (DIAS) trial[135] was a double-blind, dose-finding, placebo-controlled phase II study in which patients presenting between three and nine hours after stroke onset were treated either with the thrombolytic drug desmoteplase, or with placebo, provided that they met certain imaging criteria. Among these criteria was a requirement that a perfusion map chosen by each site in accordance with local practices demonstrated a lesion that was at least 120% of the size of the DWI lesion, as estimated by visual inspection. Favorable outcomes were seen in 22.2% of placebo-treated patients, and 60.0% of patients treated with the highest of three desmoteplase doses. Similarly positive results were achieved by the Dose Escalation of Desmoteplase for Acute Ischemic Stroke (DEDAS) trial,[136] which used the three-to-nine-hour time window, the same thrombolytic drug, and the same imaging criteria.

In the Diffusion and Perfusion Imaging Evaluation for Understanding Stroke Evolution (DEFUSE) study,[98] patients were treated with tPA between three and six hours after stroke onset. Patients underwent DWI and MR perfusion imaging before treatment, but all patients in the study were treated, regardless of their MRI findings. Reperfusion was associated with improved clinical outcomes in patients who had a significant diffusion-perfusion mismatch. However, patients without mismatch did not appear to benefit from reperfusion. In this study, perfusion lesions were defined as regions in Tmax was at least 2 sec. Significant mismatch was defined as the presence of a Tmax lesion whose size was at least 120% of the DWI lesion's size, and patients were included only if the Tmax lesion was at least 10 mL larger than the DWI lesion.

The Echoplanar Imaging Thrombolytic Evaluation Trial (EPITHET)[99] provided further evidence of the utility of perfusion imaging in expanding the therapeutic time window for thrombolysis. In EPITHET, as in DEFUSE, patients presenting between three and six hours of onset were randomized to receive either tPA or placebo. As in DEFUSE, patients underwent MRI before treatment, and MRI results were not used to select patients for treatment. Perfusion lesions were defined as in the DEFUSE trial. EPITHET's primary endpoint was assessing whether, in patients with significant DWI and perfusion lesion mismatch, tPA decreased infarct growth, compared to placebo. Although this mismatch- and treatment-related effect reached statistical significance only if patients with DWI lesions smaller than 5 cc were excluded, the effect was significant across all patients when the data were reanalyzed using a definition of mismatch volume as the volume of tissue that was included in the Tmax lesion but not in the DWI lesion, as opposed to the prespecified definition, which was the difference between the Tmax and DWI lesions volumes.[137] Treatment was associated with a significantly greater likelihood of reperfusion, and reperfusion was associated with significantly less infarct growth, and significantly better clinical outcomes.

DIAS-2[138] attempted to replicate the results of the phase II DIAS trial in a phase III study of 186 patients, by again demonstrating a clinical benefit from desmoteplase in imaging-selected patients who presented between three and nine hours after stroke onset. As in the earlier DIAS study, patients were included if they had at least a 20% mismatch between lesions presumed to represent infarct core and "penumbra." However, in DIAS-2, each site was free to follow local practice not only in choosing the method used to estimate the "penumbra," but also in choosing the method used to estimate the "core." In DIAS-2, unlike DIAS, some sites used CT rather than MRI, and therefore did not have access to DWI as an indicator of the infarct core. The DIAS-2 trial failed to show a benefit of treatment. This was speculated to be due to milder stroke population enrolled in the DIAS-2 study, low prevalence of occlusion on MRA or CTA and lower absolute mismatch volumes compared to DIAS and DEDAS studies.

The above six trials defined DWI-perfusion mismatch in different ways. They used different thresholds for mismatch, and measurements of different perfusion parameters, none of which was an indicator of underperfusion, and none of which was mentioned in the studies' abstracts. Despite these differences, five of the six trials succeeded in showing a benefit of thrombolysis outside of the usual three- or 4.5-hour time widow. It is likely that further refinements in imaging-based selection of patients for thrombolysis, perhaps incorporating multiparametric tissue modeling for even more accurate assessment of tissue risk,[139, 140] might allow for yet further expansion of the therapeutic window.

Preservation of collateral perfusion

In moderately underperfused tissue that is at risk of infarction, preservation of residual blood flow, and therefore of tissue viability, is dependent to a large degree on collateral vascular channels. In recent years, understanding of these collateral vessels has progressed, and there has been increased interest in therapeutic maneuvers that attempt to preserve or enhance the effectiveness of collateral perfusion. Techniques that may be used in the future for acute stroke treatment include external counterpulsation[141] and partial aortic occlusion,[142] which seek to augment collateral perfusion; and supplemental oxygen administration, which seeks to forestall irreversible injury by enhancing oxygen delivery when blood flow is compromised.[143] However, there is one technique for improving collateral circulation that is already in widespread use: blood pressure management.

Most acute stroke patients have elevated blood pressure.[144, 145] Although there are many possible causes for this, it may be adaptive, in that it can increase increase blood flow via narrowed arteries, and enhanced the effectiveness of collateral vascular pathways, thereby preserving threatened brain tissue. For this reason, hypertension is often allowed to remain untreated in the setting of acute stroke,[146–149] and hypertension may even be induced or augmented by pressor medications.[150–152] However, elevated blood pressure in the setting of acute stroke may also contribute to malignant brain edema,[153] increase the likelihood of hemorrhagic transformation,[154, 155] and cause serious non-neurological complications.[156]

Blood pressure management is an important issue in the management of virtually every acute stroke patient, and one that has been extensively researched. Most studies have found a U-shaped relationship between blood pressure in acute stroke and disability, with outcomes worsening if blood pressure is allowed to vary higher or lower than an optimal range.[156–158] However, in general, these studies have treated stroke patients as a somewhat homogeneous group, without distinguishing between those who do and do not have persistently hypoperfused brain tissue, a distinction that can be made by MR perfusion imaging. Presumably, the former might benefit from hypertension, whereas the latter would not, and might only suffer only the negative consequences of elevated blood pressure. One small study, incorporating 15 patients, demonstrated the effectiveness of induced hypertension therapy in patients who demonstrated a large DWI-perfusion mismatch. However, the intuitively appealing possibility of using the existence or absence of hypoperfused tissue to guide blood pressure management has yet to be tested in a large-scale trial.

Summary

In acute stroke, MR perfusion imaging can be used to measure a variety of different parameters, which provide different and complementary information about regional brain perfusion. Interpretation of MR perfusion images requires a basic qualitative understanding of the various perfusion states that may coexist in the brain of an acute stroke patient, should incorporate knowledge of several important artifacts that occur in perfusion imaging. MR perfusion imaging has been used successfully to establish the diagnosis of cerebral ischemia

in the absence of other objective evidence, and shows promise for selecting patients for thrombolytic therapy. As MR perfusion techniques undergo continuing technical refinement and are incorporated into new clinical trials, their utility in these clinical roles is likely to increase. It is also likely that MR perfusion imaging may play a larger role in guiding therapies designed to maintain and enhance collateral brain perfusion.

Acknowledgments

This work was supported in part by grant R01 NS059775 from the National Institutes of Health.

References

1. Rosen BR, Belliveau JW, Chien D. Perfusion imaging by nuclear magnetic resonance. Magn Reson Q. 1989; 5:263–281. [PubMed: 2701285]
2. Powers WJ. Cerebral hemodynamics in ischemic cerebrovascular disease. Ann Neurol. 1991; 29:231–240. [PubMed: 2042939]
3. Grubb RL Jr, Phelps ME, Ter-Pogossian MM. Regional cerebral blood volume in humans. X-ray fluorescence studies. Arch Neurol. 1973; 28:38–44. [PubMed: 4629381]
4. Grubb RL Jr, Phelps ME, Raichle ME, Ter-Pogossian MM. The effects of arterial blood pressure on the regional cerebral blood volume by x-ray fluorescence. Stroke. 1973; 4:390–399. [PubMed: 4351497]
5. Stewart GN. Researches on the circulation time in organs and on the influences which affect it, parts I–III. J Physiol (London). 1894; 15:1–89.
6. Kety SS, King BD, Horvath SM, Jeffers WS, Hafkenschiel JH. The effects of an acute reduction in blood pressure by means of differential spinal sympathetic block on the cerebral circulation of hypertensive patients. J Clin Invest. 1950; 29:402–407. [PubMed: 15415440]
7. Hossmann KA. Cerebral ischemia: Models, methods and outcomes. Neuropharmacology. 2008; 55:257–270. [PubMed: 18222496]
8. Parsons MW, Yang Q, Barber PA, Darby DG, Desmond PM, Gerraty RP, Tress BM, Davis SM. Perfusion magnetic resonance imaging maps in hyperacute stroke: Relative cerebral blood flow most accurately identifies tissue destined to infarct. Stroke. 2001; 32:1581–1587. [PubMed: 11441205]
9. Jones TH, Morawetz RB, Crowell RM, Marcoux FW, FitzGibbon SJ, DeGirolami U, Ojemann RG. Thresholds of focal cerebral ischemia in awake monkeys. J Neurosurg. 1981; 54:773–782. [PubMed: 7241187]
10. Astrup J, Siesjo B, Symon L. Thresholds in cerebral ischemia: The ischemic penumbra. Stroke. 1981; 12:723–725. [PubMed: 6272455]
11. Siesjo BK. Pathophysiology and treatment of focal cerebral ischemia. Part I: Pathophysiology. J Neurosurg. 1992; 77:169–184. [PubMed: 1625004]
12. Cordes M, Henkes H, Roll D, Eichstadt H, Christe W, Langer M, Felix R. Subacute and chronic cerebral infarctions: Spect and gadolinium-dtpa enhanced MR imaging. J Comput Assist Tomogr. 1989; 13:567–571. [PubMed: 2787339]
13. Sette G, Baron JC, Mazoyer B, Levasseur M, Pappata S, Crouzel C. Local brain haemodynamics and oxygen metabolism in cerebrovascular disease. Positron emission tomography. Brain. 1989; 112:931–951. [PubMed: 2789086]
14. Weiller C, Ringelstein EB, Reiche W, Buell U. Clinical and hemodynamic aspects of low-flow infarcts. Stroke. 1991; 22:1117–1123. [PubMed: 1926254]
15. Zaharchuk G, Mandeville JB, Bogdanov AA Jr, Weissleder R, Rosen BR, Marota JJ. Cerebrovascular dynamics of autoregulation and hypoperfusion. An MRI study of CBF and changes in total and microvascular cerebral blood volume during hemorrhagic hypotension. Stroke. 1999; 30:2197–2204. discussion 2204–2195. [PubMed: 10512929]
16. Rubin G, Firlik AD, Levy EI, Pindzola RR, Yonas H. Xenon-enhanced computed tomography cerebral blood flow measurements in acute cerebral ischemia: Review of 56 cases. J Stroke Cerebrovas Dis. 1999; 8:404–411.

17. Hakim AM, Pokrupa RP, Villanueva J, Diksic M, Evans AC, Thompson CJ, Meyer E, Yamamoto YL, Feindel WH. The effect of spontaneous reperfusion on metabolic function in early human cerebral infarcts. Ann Neurol. 1987; 21:279–289. [PubMed: 3496844]

18. Jorgensen HS, Sperling B, Nakayama H, Raaschou HO, Olsen TS. Spontaneous reperfusion of cerebral infarcts in patients with acute stroke. Incidence, time course, and clinical outcome in the copenhagen stroke study. Arch Neurol. 1994; 51:865–873. [PubMed: 8080386]

19. Bowler JV, Wade JP, Jones BE, Nijran KS, Steiner TJ. Natural history of the spontaneous reperfusion of human cerebral infarcts as assessed by 99mtc hmpao spect. J Neurol Neurosurg Psychiatry. 1998; 64:90–97. [PubMed: 9436735]

20. Marchal G, Young AR, Baron JC. Early postischemic hyperperfusion: Pathophysiologic insights from positron emission tomography. J Cereb Blood Flow Metab. 1999; 19:467–482. [PubMed: 10326714]

21. Marchal G, Furlan M, Beaudouin V, Rioux P, Hauttement JL, Serrati C, de la Sayette V, Le Doze F, Viader F, Derlon JM, Baron JC. Early spontaneous hyperperfusion after stroke. A marker of favourable tissue outcome? Brain. 1996; 119:409–419. [PubMed: 8800936]

22. Kidwell CS, Saver JL, Mattiello J, Starkman S, Vinuela F, Duckwiler G, Gobin YP, Jahan R, Vespa P, Villablanca JP, Liebeskind DS, Woods RP, Alger JR. Diffusion-perfusion MRI characterization of post-recanalization hyperperfusion in humans. Neurology. 2001; 57:2015–2021. [PubMed: 11739819]

23. Lassen NA. The luxury-perfusion syndrome and its possible relation to acute metabolic acidosis localised within the brain. Lancet. 1966; 2:1113–1115. [PubMed: 4162534]

24. Williams DS, Detre JA, Leigh JS, Koretsky AP. Magnetic resonance imaging of perfusion using spin inversion of arterial water. Proc Natl Acad Sci U S A. 1992; 89:212–216. [PubMed: 1729691]

25. Rosen BR, Belliveau JW, Vevea JM, Brady TJ. Perfusion imaging with nmr contrast agents. Magn Reson Med. 1990; 14:249–265. [PubMed: 2345506]

26. Leenders KL, Perani D, Lammertsma AA, Heather JD, Buckingham P, Healy MJ, Gibbs JM, Wise RJ, Hatazawa J, Herold S. Cerebral blood flow, blood volume and oxygen utilization. Normal values and effect of age. Brain. 1990; 113:27–47. [PubMed: 2302536]

27. Wintermark M, Albers GW, Alexandrov AV, Alger JR, Bammer R, Baron JC, Davis S, Demaerschalk BM, Derdeyn CP, Donnan GA, Eastwood JD, Fiebach JB, Fisher M, Furie KL, Goldmakher GV, Hacke W, Kidwell CS, Kloska SP, Kohrmann M, Koroshetz W, Lee TY, Lees KR, Lev MH, Liebeskind DS, Ostergaard L, Powers WJ, Provenzale J, Schellinger P, Silbergleit R, Sorensen AG, Wardlaw J, Wu O, Warach S. Acute stroke imaging research roadmap. Stroke. 2008; 39:1621–1628. [PubMed: 18403743]

28. Boxerman JL, Hamberg LM, Rosen BR, Weisskoff RM. MR contrast due to intravascular magnetic susceptibility perturbations. Magn Reson Med. 1995; 34:555–566. [PubMed: 8524024]

29. Donahue KM, Krouwer HG, Rand SD, Pathak AP, Marszalkowski CS, Censky SC, Prost RW. Utility of simultaneously acquired gradient-echo and spin-echo cerebral blood volume and morphology maps in brain tumor patients. Magn Reson Med. 2000; 43:845–853. [PubMed: 10861879]

30. Kane I, Carpenter T, Chappell F, Rivers C, Armitage P, Sandercock P, Wardlaw J. Comparison of 10 different magnetic resonance perfusion imaging processing methods in acute ischemic stroke: Effect on lesion size, proportion of patients with diffusion/perfusion mismatch, clinical scores, and radiologic outcomes. Stroke. 2007; 38:3158–3164. [PubMed: 17975106]

31. Beaulieu C, de Crespigny A, Tong DC, Moseley ME, Albers GW, Marks MP. Longitudinal magnetic resonance imaging study of perfusion and diffusion in stroke: Evolution of lesion volume and correlation with clinical outcome. Ann Neurol. 1999; 46:568–578. [PubMed: 10514093]

32. Marks MP, Tong DC, Beaulieu C, Albers GW, de Crespigny A, Moseley ME. Evaluation of early reperfusion and i.v. tPA therapy using diffusion- and perfusion-weighted MRI. Neurology. 1999; 52:1792–1798. [PubMed: 10371525]

33. Neumann-Haefelin T, Wittsack HJ, Wenserski F, Siebler M, Seitz RJ, Modder U, Freund HJ. Diffusion- and perfusion-weighted MRI. The DWI/PWI mismatch region in acute stroke. Stroke. 1999; 30:1591–1597. [PubMed: 10436106]

34. Perkins CJ, Kahya E, Roque CT, Roche PE, Newman GC. Fluid-attenuated inversion recovery and diffusion- and perfusion-weighted MRI abnormalities in 117 consecutive patients with stroke symptoms. Stroke. 2001; 32:2774–2781. [PubMed: 11739972]
35. Grandin CB, Duprez TP, Smith AM, Oppenheim C, Peeters A, Robert AR, Cosnard G. Which MR-derived perfusion parameters are the best predictors of infarct growth in hyperacute stroke? Comparative study between relative and quantitative measurements. Radiology. 2002; 223:361–370. [PubMed: 11997538]
36. Wittsack HJ, Ritzl A, Fink GR, Wenserski F, Siebler M, Seitz RJ, Modder U, Freund HJ. MR imaging in acute stroke: Diffusion-weighted and perfusion imaging parameters for predicting infarct size. Radiology. 2002; 222:397–403. [PubMed: 11818605]
37. Derex L, Nighoghossian N, Hermier M, Adeleine P, Berthezene Y, Philippeau F, Honnorat J, Froment JC, Trouillas P. Influence of pretreatment MRI parameters on clinical outcome, recanalization and infarct size in 49 stroke patients treated by intravenous tissue plasminogen activator. J Neurol Sci. 2004; 225:3–9. [PubMed: 15465079]
38. Yamada K, Wu O, Gonzalez RG, Bakker D, Østergaard L, Copen WA, Weisskoff RM, Rosen BR, Yagi K, Nishimura T, Sorensen AG. Magnetic resonance perfusion-weighted imaging of acute cerebral infarction: Effect of the calculation methods and underlying vasculopathy. Stroke. 2002; 33:87–94. [PubMed: 11779894]
39. Ribo M, Molina CA, Rovira A, Quintana M, Delgado P, Montaner J, Grive E, Arenillas JF, Alvarez-Sabin J. Safety and efficacy of intravenous tissue plasminogen activator stroke treatment in the 3- to 6-hour window using multimodal transcranial Doppler/MRI selection protocol. Stroke. 2005; 36:602–606. [PubMed: 15692107]
40. Cenic A, Nabavi DG, Craen RA, Gelb AW, Lee TY. Dynamic CT measurement of cerebral blood flow: A validation study. AJNR: American Journal of Neuroradiology. 1999; 20:63–73. [PubMed: 9974059]
41. Nabavi DG, Cenic A, Dool J, Smith RM, Espinosa F, Craen RA, Gelb AW, Lee TY. Quantitative assessment of cerebral hemodynamics using CT: Stability, accuracy, and precision studies in dogs. J Comput Assist Tomogr. 1999; 23:506–515. [PubMed: 10433275]
42. Wintermark M, Thiran JP, Maeder P, Schnyder P, Meuli R. Simultaneous measurement of regional cerebral blood flow by perfusion CT and stable xenon CT: A validation study. AJNR: American Journal of Neuroradiology. 2001; 22:905–914. [PubMed: 11337336]
43. Gillard JH, Antoun NM, Burnet NG, Pickard JD. Reproducibility of quantitative CT perfusion imaging. Br J Radiol. 2001; 74:552–555. [PubMed: 11459735]
44. Furukawa M, Kashiwagi S, Matsunaga N, Suzuki M, Kishimoto K, Shirao S. Evaluation of cerebral perfusion parameters measured by perfusion CT in chronic cerebral ischemia: Comparison with xenon CT. J Comput Assist Tomogr. 2002; 26:272–278. [PubMed: 11884786]
45. Rempp KA, Brix G, Wenz F, Becker CR, Guckel F, Lorenz WJ. Quantification of regional cerebral blood flow and volume with dynamic susceptibility contrast-enhanced MR imaging. Radiology. 1994; 193:637–641. [PubMed: 7972800]
46. Østergaard L, Smith DF, Vestergaard-Poulsen P, Hansen SB, Gee AD, Gjedde A, Gyldensted C. Absolute cerebral blood flow and blood volume measured by magnetic resonance imaging bolus tracking: Comparison with positron emission tomography values. J Cereb Blood Flow Metab. 1998; 18:425–432. [PubMed: 9538908]
47. Hagen T, Bartylla K, Piepgras U. Correlation of regional cerebral blood flow measured by stable xenon CT and perfusion MRI. J Comput Assist Tomogr. 1999; 23:257–264. [PubMed: 10096334]
48. Sakoh M, Rohl L, Gyldensted C, Gjedde A, Østergaard L. Cerebral blood flow and blood volume measured by magnetic resonance imaging bolus tracking after acute stroke in pigs: Comparison with [(15)o]h(2)o positron emission tomography. Stroke. 2000; 31:1958–1964. [PubMed: 10926964]
49. Smith AM, Grandin CB, Duprez T, Mataigne F, Cosnard G. Whole brain quantitative CBF, CBV, and MTT measurements using MRI bolus tracking: Implementation and application to data acquired from hyperacute stroke patients. J Magn Reson Imaging. 2000; 12:400–410. [PubMed: 10992307]

50. Lin W, Celik A, Derdeyn C, An H, Lee Y, Videen T, Østergaard L, Powers WJ. Quantitative measurements of cerebral blood flow in patients with unilateral carotid artery occlusion: A pet and MR study. J Magn Reson Imaging. 2001; 14:659–667. [PubMed: 11747021]
51. Endo H, Inoue T, Ogasawara K, Fukuda T, Kanbara Y, Ogawa A. Quantitative assessment of cerebral hemodynamics using perfusion-weighted MRI in patients with major cerebral artery occlusive disease: Comparison with positron emission tomography. Stroke. 2006; 37:388–392. [PubMed: 16373637]
52. Sorensen AG, Buonanno FS, Gonzalez RG, Schwamm LH, Lev MH, Huang-Hellinger FR, Reese TG, Weisskoff RM, Davis TL, Suwanwela N, Can U, Moreira JA, Copen WA, Look RB, Finklestein SP, Rosen BR, Koroshetz WJ. Hyperacute stroke: Evaluation with combined multisection diffusion-weighted and hemodynamically weighted echo-planar MR imaging. Radiology. 1996; 199:391–401. [PubMed: 8668784]
53. Rordorf G, Koroshetz WJ, Copen WA, Cramer SC, Schaefer PW, Budzik RF Jr, Schwamm LH, Buonanno F, Sorensen AG, Gonzalez G. Regional ischemia and ischemic injury in patients with acute middle cerebral artery stroke as defined by early diffusion-weighted and perfusion-weighted MRI. Stroke. 1998; 29:939–943. [PubMed: 9596239]
54. Ueda T, Yuh WT, Maley JE, Quets JP, Hahn PY, Magnotta VA. Outcome of acute ischemic lesions evaluated by diffusion and perfusion MR imaging. AJNR: American Journal of Neuroradiology. 1999; 20:983–989. [PubMed: 10445433]
55. Sorensen AG, Copen WA, Østergaard L, Buonanno FS, Gonzalez RG, Rordorf G, Rosen BR, Schwamm LH, Weisskoff RM, Koroshetz WJ. Hyperacute stroke: Simultaneous measurement of relative cerebral blood volume, relative cerebral blood flow, and mean tissue transit time. Radiology. 1999; 210:519–527. [PubMed: 10207439]
56. Karonen JO, Liu Y, Vanninen RL, Østergaard L, Kaarina Partanen PL, Vainio PA, Vanninen EJ, Nuutinen J, Roivainen R, Soimakallio S, Kuikka JT, Aronen HJ. Combined perfusion- and diffusion-weighted MR imaging in acute ischemic stroke during the 1st week: A longitudinal study. Radiology. 2000; 217:886–894. [PubMed: 11110958]
57. Schaefer PW, Hunter GJ, He J, Hamberg LM, Sorensen AG, Schwamm LH, Koroshetz WJ, Gonzalez RG. Predicting cerebral ischemic infarct volume with diffusion and perfusion MR imaging. AJNR: American Journal of Neuroradiology. 2002; 23:1785–1794. [PubMed: 12427640]
58. Wintermark M. Brain perfusion-CT in acute stroke patients. Eur Radiol. 2005; 15 (Suppl 4):D28–31. [PubMed: 16479642]
59. Nagar VA, McKinney AM, Karagulle AT, Truwit CL. Reperfusion phenomenon masking acute and subacute infarcts at dynamic perfusion CT: Confirmation by fusion of CT and diffusion-weighted MR images. AJR Am J Roentgenol. 2009; 193:1629–1638. [PubMed: 19933658]
60. Benner T, Heiland S, Erb G, Forsting M, Sartor K. Accuracy of gamma-variate fits to concentration-time curves from dynamic susceptibility-contrast enhanced MRI: Influence of time resolution, maximal signal drop and signal-to-noise. Magn Reson Imaging. 1997; 15:307–317. [PubMed: 9201678]
61. Lin W, Celik A, Paczynski RP. Regional cerebral blood volume: A comparison of the dynamic imaging and the steady state methods. J Magn Reson Imaging. 1999; 9:44–52. [PubMed: 10030649]
62. deIpolyi, AR.; Wu, O.; Schaefer, PW.; Macklin, EA.; Schwamm, LH.; Ackerman, RH.; Gonzalez, RG.; Copen, WA. Cerebral blood volume measurements in acute ischemic stroke are technique-dependent and cannot substitute for DWI. American Society for Neuroradiology 48th Annual Meeting; 2010.
63. Kwong KK, Reese TG, Nelissen K, Wu O, Chan ST, Benner T, Mandeville JB, Foley M, Vanduffel W, Chesler DA. Early time points perfusion imaging. Neuroimage. 2011; 54:1070–1082. [PubMed: 20851196]
64. King RB, Deussen A, Raymond GM, Bassingthwaighte JB. A vascular transport operator. Am J Physiol. 1993; 265:H2196–2208. [PubMed: 8285259]
65. van Osch MJ, Vonken EJ, Wu O, Viergever MA, van der Grond J, Bakker CJ. Model of the human vasculature for studying the influence of contrast injection speed on cerebral perfusion MRI. Magn Reson Med. 2003; 50:614–622. [PubMed: 12939770]

66. Rausch M, Scheffler K, Rudin M, Radu EW. Analysis of input functions from different arterial branches with gamma variate functions and cluster analysis for quantitative blood volume measurements. Magn Reson Imaging. 2000; 18:1235–1243. [PubMed: 11167043]

67. Carroll TJ, Rowley HA, Haughton VM. Automatic calculation of the arterial input function for cerebral perfusion imaging with MR imaging. Radiology. 2003; 227:593–600. [PubMed: 12663823]

68. Mouridsen K, Christensen S, Gyldensted L, Ostergaard L. Automatic selection of arterial input function using cluster analysis. Magn Reson Med. 2006; 55:524–531. [PubMed: 16453314]

69. Østergaard L, Weisskoff RM, Chesler DA, Gyldensted C, Rosen BR. High resolution measurement of cerebral blood flow using intravascular tracer bolus passages. Part I: Mathematical approach and statistical analysis. Magn Reson Med. 1996; 36:715–725. [PubMed: 8916022]

70. Østergaard L, Sorensen AG, Kwong KK, Weisskoff RM, Gyldensted C, Rosen BR. High resolution measurement of cerebral blood flow using intravascular tracer bolus passages. Part II: Experimental comparison and preliminary results. Magn Reson Med. 1996; 36:726–736. [PubMed: 8916023]

71. Kudo K, Sasaki M, Yamada K, Momoshima S, Utsunomiya H, Shirato H, Ogasawara K. Differences in CT perfusion maps generated by different commercial software: Quantitative analysis by using identical source data of acute stroke patients. Radiology. 2010; 254:200–209. [PubMed: 20032153]

72. Calamante F, Gadian DG, Connelly A. Delay and dispersion effects in dynamic susceptibility contrast MRI: Simulations using singular value decomposition. Magn Reson Med. 2000; 44:466–473. [PubMed: 10975900]

73. Calamante F, Gadian DG, Connelly A. Quantification of perfusion using bolus tracking magnetic resonance imaging in stroke: Assumptions, limitations, and potential implications for clinical use. Stroke. 2002; 33:1146–1151. [PubMed: 11935075]

74. Wu O, Østergaard L, Koroshetz WJ, Schwamm LH, O'Donnell J, Schaefer PW, Rosen BR, Weisskoff RM, Sorensen AG. Effects of tracer arrival time on flow estimates in MR perfusion-weighted imaging. Magn Reson Med. 2003; 50:856–864. [PubMed: 14523973]

75. Lythgoe DJ, Ostergaard L, William SC, Cluckie A, Buxton-Thomas M, Simmons A, Markus HS. Quantitative perfusion imaging in carotid artery stenosis using dynamic susceptibility contrast-enhanced magnetic resonance imaging. Magn Reson Imaging. 2000; 18:1–11. [PubMed: 10642097]

76. Calamante F, Morup M, Hansen LK. Defining a local arterial input function for perfusion MRI using independent component analysis. Magn Reson Med. 2004; 52:789–797. [PubMed: 15389944]

77. Lorenz C, Benner T, Lopez CJ, Ay H, Zhu MW, Aronen H, Karonen J, Liu Y, Nuutinen J, Sorensen AG. Effect of using local arterial input functions on cerebral blood flow estimation. J Magn Reson Imaging. 2006; 24:57–65. [PubMed: 16767708]

78. Lorenz C, Benner T, Chen PJ, Lopez CJ, Ay H, Zhu MW, Menezes NM, Aronen H, Karonen J, Liu Y, Nuutinen J, Sorensen AG. Automated perfusion-weighted MRI using localized arterial input functions. J Magn Reson Imaging. 2006; 24:1133–1139. [PubMed: 16969793]

79. Christensen S, Mouridsen K, Wu O, Hjort N, Karstoft H, Thomalla G, Rother J, Fiehler J, Kucinski T, Ostergaard L. Comparison of 10 perfusion MRI parameters in 97 sub-6-hour stroke patients using voxel-based receiver operating characteristics analysis. Stroke. 2009; 40:2055–2061. [PubMed: 19359626]

80. Lee JJ, Bretthorst GL, Derdeyn CP, Powers WJ, Videen TO, Snyder AZ, Markham J, Shimony JS. Dynamic susceptibility contrast MRI with localized arterial input functions. Magn Reson Med. 2010; 63:1305–1314. [PubMed: 20432301]

81. Duhamel G, Schlaug G, Alsop DC. Measurement of arterial input functions for dynamic susceptibility contrast magnetic resonance imaging using echoplanar images: Comparison of physical simulations with in vivo results. Magn Reson Med. 2006; 55:514–523. [PubMed: 16463343]

82. Bleeker EJ, van Buchem MA, van Osch MJ. Optimal location for arterial input function measurements near the middle cerebral artery in first-pass perfusion MRI. J Cereb Blood Flow Metab. 2009; 29:840–852. [PubMed: 19142193]

83. Rose SE, Janke AL, Griffin M, Strudwick MW, Finnigan S, Semple J, Chalk JB. Improving the prediction of final infarct size in acute stroke with bolus delay-corrected perfusion MRI measures. J Magn Reson Imaging. 2004; 20:941–947. [PubMed: 15558572]

84. Rose SE, Janke AL, Griffin M, Finnigan S, Chalk JB. Improved prediction of final infarct volume using bolus delay-corrected perfusion-weighted MRI: Implications for the ischemic penumbra. Stroke. 2004; 35:2466–2471. [PubMed: 15472086]

85. Wu O, Østergaard L, Weisskoff RM, Benner T, Rosen BR, Sorensen AG. Tracer arrival timing-insensitive technique for estimating flow in MR perfusion-weighted imaging using singular value decomposition with a block-circulant deconvolution matrix. Magn Reson Med. 2003; 50:164–174. [PubMed: 12815691]

86. Baird AE, Benfield A, Schlaug G, Siewert B, Lovblad KO, Edelman RR, Warach S. Enlargement of human cerebral ischemic lesion volumes measured by diffusion-weighted magnetic resonance imaging. Ann Neurol. 1997; 41:581–589. [PubMed: 9153519]

87. Grandin CB, Duprez TP, Smith AM, Mataigne F, Peeters A, Oppenheim C, Cosnard G. Usefulness of magnetic resonance-derived quantitative measurements of cerebral blood flow and volume in prediction of infarct growth in hyperacute stroke. Stroke. 2001; 32:1147–1153. [PubMed: 11340224]

88. Fink JN, Kumar S, Horkan C, Linfante I, Selim MH, Caplan LR, Schlaug G. The stroke patient who woke up: Clinical and radiological features, including diffusion and perfusion MRI. Stroke. 2002; 33:988–993. [PubMed: 11935049]

89. Coutts SB, Simon JE, Tomanek AI, Barber PA, Chan J, Hudon ME, Mitchell JR, Frayne R, Eliasziw M, Buchan AM, Demchuk AM. Reliability of assessing percentage of diffusion-perfusion mismatch. Stroke. 2003; 34:1681–1683. [PubMed: 12805485]

90. Ay H, Koroshetz WJ, Vangel M, Benner T, Melinosky C, Zhu M, Menezes N, Lopez CJ, Sorensen AG. Conversion of ischemic brain tissue into infarction increases with age. Stroke. 2005; 36:2632–2636. [PubMed: 16269639]

91. Yoo AJ, Barak ER, Copen WA, Kamalian S, Gharai LR, Pervez MA, Schwamm LH, Gonzalez RG, Schaefer PW. Combining acute diffusion-weighted imaging and mean transmit time lesion volumes with national institutes of health stroke scale score improves the prediction of acute stroke outcome. Stroke. 2010; 41:1728–1735. [PubMed: 20595665]

92. Rivers CS, Wardlaw JM, Armitage PA, Bastin ME, Carpenter TK, Cvoro V, Hand PJ, Dennis MS. Do acute diffusion- and perfusion-weighted MRI lesions identify final infarct volume in ischemic stroke? Stroke. 2006; 37:98–104. [PubMed: 16322499]

93. Shih LC, Saver JL, Alger JR, Starkman S, Leary MC, Vinuela F, Duckwiler G, Gobin YP, Jahan R, Villablanca JP, Vespa PM, Kidwell CS. Perfusion-weighted magnetic resonance imaging thresholds identifying core, irreversibly infarcted tissue. Stroke. 2003; 34:1425–1430. [PubMed: 12738899]

94. Olivot JM, Mlynash M, Thijs VN, Kemp S, Lansberg MG, Wechsler L, Bammer R, Marks MP, Albers GW. Optimal Tmax threshold for predicting penumbral tissue in acute stroke. Stroke. 2009; 40:469–475. [PubMed: 19109547]

95. Bang OY, Lee KH, Kim SJ, Liebeskind DS. Benign oligemia despite a malignant MRI profile in acute ischemic stroke. J Clin Neurol. 2010; 6:41–45. [PubMed: 20386643]

96. Kidwell CS, Saver JL, Mattiello J, Starkman S, Vinuela F, Duckwiler G, Gobin YP, Jahan R, Vespa P, Kalafut M, Alger JR. Thrombolytic reversal of acute human cerebral ischemic injury shown by diffusion/perfusion magnetic resonance imaging. Ann Neurol. 2000; 47:462–469. [PubMed: 10762157]

97. Kakuda W, Lansberg MG, Thijs VN, Kemp SM, Bammer R, Wechsler LR, Moseley ME, Marks MP, Albers GW, Investigators D. Optimal definition for PWI/DWI mismatch in acute ischemic stroke patients. J Cereb Blood Flow Metab. 2008; 28:887–891. [PubMed: 18183031]

98. Albers GW, Thijs VN, Wechsler L, Kemp S, Schlaug G, Skalabrin E, Bammer R, Kakuda W, Lansberg MG, Shuaib A, Coplin W, Hamilton S, Moseley M, Marks MP. Magnetic resonance

imaging profiles predict clinical response to early reperfusion: The diffusion and perfusion imaging evaluation for understanding stroke evolution (DEFUSE) study. Ann Neurol. 2006; 60:508–517. [PubMed: 17066483]

99. Davis SM, Donnan GA, Parsons MW, Levi C, Butcher KS, Peeters A, Barber PA, Bladin C, De Silva DA, Byrnes G, Chalk JB, Fink JN, Kimber TE, Schultz D, Hand PJ, Frayne J, Hankey G, Muir K, Gerraty R, Tress BM, Desmond PM, Investigators E. Effects of alteplase beyond 3 h after stroke in the echoplanar imaging thrombolytic evaluation trial (EPITHET): A placebo-controlled randomised trial. Lancet Neurol. 2008; 7:209–309.
100. Liebeskind DS. Collaterals in acute stroke: Beyond the clot. Neuroimaging Clin N Am. 2005; 15:553–573. x. [PubMed: 16360589]
101. Christensen S, Calamante F, Hjort N, Wu O, Blankholm AD, Desmond P, Davis S, Ostergaard L. Inferring origin of vascular supply from tracer arrival timing patterns using bolus tracking MRI. J Magn Reson Imaging. 2008; 27:1371–1381. [PubMed: 18504757]
102. Lövblad KO, Laubach HJ, Baird AE, Curtin F, Schlaug G, Edelman RR, Warach S. Clinical experience with diffusion-weighted MR in patients with acute stroke. AJNR: American Journal of Neuroradiology. 1998; 19:1061–1066. [PubMed: 9672012]
103. Singer MB, Chong J, Lu D, Schonewille WJ, Tuhrim S, Atlas SW. Diffusion-weighted MRI in acute subcortical infarction. Stroke. 1998; 29:133–136. [PubMed: 9445341]
104. van Everdingen KJ, van der Grond J, Kappelle LJ, Ramos LM, Mali WP. Diffusion-weighted magnetic resonance imaging in acute stroke. Stroke. 1998; 29:1783–1790. [PubMed: 9731595]
105. Gonzalez RG, Schaefer PW, Buonanno FS, Schwamm LH, Budzik RF, Rordorf G, Wang B, Sorensen AG, Koroshetz WJ. Diffusion-weighted MR imaging: Diagnostic accuracy in patients imaged within 6 hours of stroke symptom onset. Radiology. 1999; 210:155–162. [PubMed: 9885601]
106. Urbach H, Flacke S, Keller E, Textor J, Berlis A, Hartmann A, Reul J, Solymosi L, Schild HH. Detectability and detection rate of acute cerebral hemisphere infarcts on CT and diffusion-weighted MRI. Neuroradiology. 2000; 42:722–727. [PubMed: 11110072]
107. Fiebach JB, Schellinger PD, Jansen O, Meyer M, Wilde P, Bender J, Schramm P, Juttler E, Oehler J, Hartmann M, Hahnel S, Knauth M, Hacke W, Sartor K. CT and diffusion-weighted MR imaging in randomized order: Diffusion- weighted imaging results in higher accuracy and lower interrater variability in the diagnosis of hyperacute ischemic stroke. Stroke. 2002; 33:2206–2210. [PubMed: 12215588]
108. Mullins ME, Schaefer PW, Sorensen AG, Halpern EF, Ay H, He J, Koroshetz WJ, Gonzalez RG. CT and conventional and diffusion-weighted MR imaging in acute stroke: Study in 691 patients at presentation to the emergency department. Radiology. 2002; 224:353–360. [PubMed: 12147827]
109. Hand PJ, Kwan J, Lindley RI, Dennis MS, Wardlaw JM. Distinguishing between stroke and mimic at the bedside: The brain attack study. Stroke. 2006; 37:769–775. [PubMed: 16484610]
110. Johnston SC, Gress DR, Browner WS, Sidney S. Short-term prognosis after emergency department diagnosis of TIA. JAMA. 2000; 284:2901–2906. [PubMed: 11147987]
111. Furie KL, Kasner SE, Adams RJ, Albers GW, Bush RL, Fagan SC, Halperin JL, Johnston SC, Katzan I, Kernan WN, Mitchell PH, Ovbiagele B, Palesch YY, Sacco RL, Schwamm LH, Wassertheil-Smoller S, Turan TN, Wentworth D. Guidelines for the prevention of stroke in patients with stroke or transient ischemic attack. A guideline for healthcare professionals from the american heart association/american stroke association. Stroke. 2010
112. Coutts SB, Sylaja PN, Choi YB, Al-Khathami A, Sivakumar C, Jeerakathil TJ, Sarma PS, Hill MD. The aspire approach for TIA risk stratification. Can J Neurol Sci. 2011; 38:78–81. [PubMed: 21156434]
113. Ovbiagele B, Kidwell CS, Saver JL. Epidemiological impact in the united states of a tissue-based definition of transient ischemic attack. Stroke. 2003; 34:919–924. [PubMed: 12637701]
114. Restrepo L, Jacobs MA, Barker PB, Wityk RJ. Assessment of transient ischemic attack with diffusion- and perfusion-weighted imaging. AJNR: American Journal of Neuroradiology. 2004; 25:1645–1652. [PubMed: 15569725]

115. Krol AL, Coutts SB, Simon JE, Hill MD, Sohn CH, Demchuk AM, Group VS. Perfusion MRI abnormalities in speech or motor transient ischemic attack patients. Stroke. 2005; 36:2487–2489. [PubMed: 16224075]

116. Mlynash M, Olivot JM, Tong DC, Lansberg MG, Eyngorn I, Kemp S, Moseley ME, Albers GW. Yield of combined perfusion and diffusion MR imaging in hemispheric TIA. Neurology. 2009; 72:1127–1133. [PubMed: 19092109]

117. NINDS rt-PA Study Group. Tissue plasminogen activator for acute ischemic stroke. The national institute of neurological disorders and stroke rt-PA stroke study group. N Engl J Med. 1995; 333:1581–1587. [PubMed: 7477192]

118. Hacke W, Kaste M, Fieschi C, Toni D, Lesaffre E, von Kummer R, Boysen G, Bluhmki E, Hoxter G, Mahagne MH. Intravenous thrombolysis with recombinant tissue plasminogen activator for acute hemispheric stroke. The european cooperative acute stroke study (ECASS). JAMA. 1995; 274:1017–1025. [PubMed: 7563451]

119. Hacke W, Kaste M, Fieschi C, von Kummer R, Davalos A, Meier D, Larrue V, Bluhmki E, Davis S, Donnan G, Schneider D, Diez-Tejedor E, Trouillas P. Randomised double-blind placebo-controlled trial of thrombolytic therapy with intravenous alteplase in acute ischaemic stroke (ECASS II). Second european-australasian acute stroke study investigators. Lancet. 1998; 352:1245–1251. [PubMed: 9788453]

120. Clark WM, Wissman S, Albers GW, Jhamandas JH, Madden KP, Hamilton S. Recombinant tissue-type plasminogen activator (Alteplase) for ischemic stroke 3 to 5 hours after symptom onset. The atlantis study: A randomized controlled trial. Alteplase thrombolysis for acute noninterventional therapy in ischemic stroke. JAMA. 1999; 282:2019–2026. [PubMed: 10591384]

121. Wahlgren N, Ahmed N, Davalos A, Ford GA, Grond M, Hacke W, Hennerici MG, Kaste M, Kuelkens S, Larrue V, Lees KR, Roine RO, Soinne L, Toni D, Vanhooren G, investigators S-M. Thrombolysis with alteplase for acute ischaemic stroke in the safe implementation of thrombolysis in stroke-monitoring study (SITS-MOST): An observational study. Lancet. 2007; 369:275–282. [PubMed: 17258667]

122. Bluhmki E, Chamorro A, Davalos A, Machnig T, Sauce C, Wahlgren N, Wardlaw J, Hacke W. Stroke treatment with alteplase given 3.0–4.5 h after onset of acute ischaemic stroke (ECASS III): Additional outcomes and subgroup analysis of a randomised controlled trial. Lancet Neurol. 2009; 8:1095–1102. [PubMed: 19850525]

123. Boode B, Welzen V, Franke C, van Oostenbrugge R. Estimating the number of stroke patients eligible for thrombolytic treatment if delay could be avoided. Cerebrovasc Dis. 2007; 23:294–298. [PubMed: 17199087]

124. Smith MA, Doliszny KM, Shahar E, McGovern PG, Arnett DK, Luepker RV. Delayed hospital arrival for acute stroke: The Minnesota stroke survey. Ann Intern Med. 1998; 129:190–196. [PubMed: 9696726]

125. Katzan IL, Furlan AJ, Lloyd LE, Frank JI, Harper DL, Hinchey JA, Hammel JP, Qu A, Sila CA. Use of tissue-type plasminogen activator for acute ischemic stroke: The Cleveland area experience. JAMA. 2000; 283:1151–1158. [PubMed: 10703777]

126. Barber PA, Zhang J, Demchuk AM, Hill MD, Buchan AM. Why are stroke patients excluded from TPA therapy? An analysis of patient eligibility. Neurology. 2001; 56:1015–1020. [PubMed: 11320171]

127. O'Connor RE, McGraw P, Edelsohn L. Thrombolytic therapy for acute ischemic stroke: Why the majority of patients remain ineligible for treatment. Ann Emerg Med. 1999; 33:9–14. [PubMed: 9867881]

128. Wu O, Schwamm LH, Sorensen AG. Imaging stroke patients with unclear onset times. Neuroimaging Clin N Am. 2011 in press.

129. Tong DC, Yenari MA, Albers GW, O'Brien M, Marks MP, Moseley ME. Correlation of perfusion- and diffusion-weighted MRI with nihss score in acute (<6.5 hour) ischemic stroke. Neurology. 1998; 50:864–870. [PubMed: 9566364]

130. Karonen JO, Vanninen RL, Liu Y, Østergaard L, Kuikka JT, Nuutinen J, Vanninen EJ, Partanen PL, Vainio PA, Korhonen K, Perkio J, Roivainen R, Sivenius J, Aronen HJ. Combined diffusion

and perfusion MRI with correlation to single-photon emission CT in acute ischemic stroke. Ischemic penumbra predicts infarct growth. Stroke. 1999; 30:1583–1590. [PubMed: 10436105]

131. Parsons MW, Barber PA, Chalk J, Darby DG, Rose S, Desmond PM, Gerraty RP, Tress BM, Wright PM, Donnan GA, Davis SM. Diffusion- and perfusion-weighted MRI response to thrombolysis in stroke. Ann Neurol. 2002; 51:28–37. [PubMed: 11782981]
132. Grant PE, He J, Halpern EF, Wu O, Schaefer PW, Schwamm LH, Budzik RF, Sorensen AG, Koroshetz WJ, Gonzalez RG. Frequency and clinical context of decreased apparent diffusion coefficient reversal in the human brain. Radiology. 2001; 221:43–50. [PubMed: 11568319]
133. Barber PA, Darby DG, Desmond PM, Yang Q, Gerraty RP, Jolley D, Donnan GA, Tress BM, Davis SM. Prediction of stroke outcome with echoplanar perfusion- and diffusion-weighted MRI. Neurology. 1998; 51:418–426. [PubMed: 9710013]
134. Schlaug G, Benfield A, Baird AE, Siewert B, Lovblad KO, Parker RA, Edelman RR, Warach S. The ischemic penumbra: Operationally defined by diffusion and perfusion MRI. Neurology. 1999; 53:1528–1537. [PubMed: 10534263]
135. Hacke W, Albers G, Al-Rawi Y, Bogousslavsky J, Davalos A, Eliasziw M, Fischer M, Furlan A, Kaste M, Lees KR, Soehngen M, Warach S, Group DS. The desmoteplase in acute ischemic stroke trial (DIAS): A phase II MRI-based 9-hour window acute stroke thrombolysis trial with intravenous desmoteplase. Stroke. 2005; 36:66–73. [PubMed: 15569863]
136. Furlan AJ, Eyding D, Albers GW, Al-Rawi Y, Lees KR, Rowley HA, Sachara C, Soehngen M, Warach S, Hacke W, Investigators D. Dose escalation of desmoteplase for acute ischemic stroke (DEDAS): Evidence of safety and efficacy 3 to 9 hours after stroke onset. Stroke. 2006; 37:1227–1231. [PubMed: 16574922]
137. Nagakane Y, Christensen S, Brekenfeld C, Ma H, Churilov L, Parsons MW, Levi CR, Butcher KS, Peeters A, Barber PA, Bladin CF, De Silva DA, Fink J, Kimber TE, Schultz DW, Muir KW, Tress BM, Desmond PM, Davis SM, Donnan GA. EPITHET: Positive result after reanalysis using baseline diffusion-weighted imaging/perfusion-weighted imaging co-registration. Stroke. 2011; 42:59–64. [PubMed: 21127303]
138. Hacke W, Furlan AJ, Al-Rawi Y, Davalos A, Fiebach JB, Gruber F, Kaste M, Lipka LJ, Pedraza S, Ringleb PA, Rowley HA, Schneider D, Schwamm LH, Leal JS, Sohngen M, Teal PA, Wilhelm-Ogunbiyi K, Wintermark M, Warach S. Intravenous desmoteplase in patients with acute ischaemic stroke selected by MRI perfusion-diffusion weighted imaging or perfusion CT (DIAS-2): A prospective, randomised, double-blind, placebo-controlled study. Lancet Neurol. 2009; 8:141–150. [PubMed: 19097942]
139. Rose SE, Chalk JB, Griffin MP, Janke AL, Chen F, McLachan GJ, Peel D, Zelaya FO, Markus HS, Jones DK, Simmons A, O'Sullivan M, Jarosz JM, Strugnell W, Doddrell DM, Semple J. MRI based diffusion and perfusion predictive model to estimate stroke evolution. Magn Reson Imaging. 2001; 19:1043–1053. [PubMed: 11711228]
140. Wu O, Koroshetz WJ, Østergaard L, Buonanno FS, Copen WA, Gonzalez RG, Rordorf G, Rosen BR, Schwamm LH, Weisskoff RM, Sorensen AG. Predicting tissue outcome in acute human cerebral ischemia using combined diffusion- and perfusion-weighted MR imaging. Stroke. 2001; 32:933–942. [PubMed: 11283394]
141. Han JH, Wong KS. Is counterpulsation a potential therapy for ischemic stroke? Cerebrovasc Dis. 2008; 26:97–105. [PubMed: 18560211]
142. Uflacker R, Schonholz C, Papamitisakis N. Interim report of the SENTIS trial: Cerebral perfusion augmentation via partial aortic occlusion in acute ischemic stroke. J Cardiovasc Surg (Torino). 2008; 49:715–721.
143. Singhal AB, Benner T, Roccatagliata L, Koroshetz WJ, Schaefer PW, Lo EH, Buonanno FS, Gonzalez RG, Sorensen AG. A pilot study of normobaric oxygen therapy in acute ischemic stroke. Stroke. 2005; 36:797–802. [PubMed: 15761201]
144. International Stroke Trial Collaborative Group. The international stroke trial (IST): A randomised trial of aspirin, subcutaneous heparin, both, or neither among 19435 patients with acute ischaemic stroke. International stroke trial collaborative group. Lancet. 1997; 349:1569–1581. [PubMed: 9174558]

145. CAST (Chinese Acute Stroke Trial) Collaborative Group. CAST: Randomised placebo-controlled trial of early aspirin use in 20,000 patients with acute ischaemic stroke. CAST (chinese acute stroke trial) collaborative group. Lancet. 1997; 349:1641–1649. [PubMed: 9186381]

146. Barer DH, Cruickshank JM, Ebrahim SB, Mitchell JR. Low dose beta blockade in acute stroke ("BEST" trial): An evaluation. Br Med J (Clin Res Ed). 1988; 296:737–741.

147. Ahmed N, Nasman P, Wahlgren NG. Effect of intravenous nimodipine on blood pressure and outcome after acute stroke. Stroke. 2000; 31:1250–1255. [PubMed: 10835440]

148. Horn J, Limburg M. Calcium antagonists for ischemic stroke: A systematic review. Stroke. 2001; 32:570–576. [PubMed: 11157199]

149. Ahmed N, Wahlgren NG. Effects of blood pressure lowering in the acute phase of total anterior circulation infarcts and other stroke subtypes. Cerebrovasc Dis. 2003; 15:235–243. [PubMed: 12686786]

150. Rordorf G, Cramer SC, Efird JT, Schwamm LH, Buonanno F, Koroshetz WJ. Pharmacological elevation of blood pressure in acute stroke. Clinical effects and safety. Stroke. 1997; 28:2133–2138. [PubMed: 9368553]

151. Hillis AE, Ulatowski JA, Barker PB, Torbey M, Ziai W, Beauchamp NJ, Oh S, Wityk RJ. A pilot randomized trial of induced blood pressure elevation: Effects on function and focal perfusion in acute and subacute stroke. Cerebrovasc Dis. 2003; 16:236–246. [PubMed: 12865611]

152. Mistri AK, Robinson TG, Potter JF. Pressor therapy in acute ischemic stroke: Systematic review. Stroke. 2006; 37:1565–1571. [PubMed: 16675735]

153. Krieger DW, Demchuk AM, Kasner SE, Jauss M, Hantson L. Early clinical and radiological predictors of fatal brain swelling in ischemic stroke. Stroke. 1999; 30:287–292. [PubMed: 9933261]

154. Bowes MP, Zivin JA, Thomas GR, Thibodeaux H, Fagan SC. Acute hypertension, but not thrombolysis, increases the incidence and severity of hemorrhagic transformation following experimental stroke in rabbits. Exp Neurol. 1996; 141:40–46. [PubMed: 8797666]

155. Fagan SC, Bowes MP, Lyden PD, Zivin JA. Acute hypertension promotes hemorrhagic transformation in a rabbit embolic stroke model: Effect of labetalol. Exp Neurol. 1998; 150:153–158. [PubMed: 9514832]

156. Vemmos KN, Spengos K, Tsivgoulis G, Zakopoulos N, Manios E, Kotsis V, Daffertshofer M, Vassilopoulos D. Factors influencing acute blood pressure values in stroke subtypes. J Hum Hypertens. 2004; 18:253–259. [PubMed: 15037874]

157. Okumura K, Ohya Y, Maehara A, Wakugami K, Iseki K, Takishita S. Effects of blood pressure levels on case fatality after acute stroke. J Hypertens. 2005; 23:1217–1223. [PubMed: 15894898]

158. Ahmed N, Wahlgren N, Brainin M, Castillo J, Ford GA, Kaste M, Lees KR, Toni D. Relationship of blood pressure, antihypertensive therapy, and outcome in ischemic stroke treated with intravenous thrombolysis: Retrospective analysis from safe implementation of thrombolysis in stroke-international stroke thrombolysis register (SITS-ISTR). Stroke. 2009; 40:2442–2449. [PubMed: 19461022]

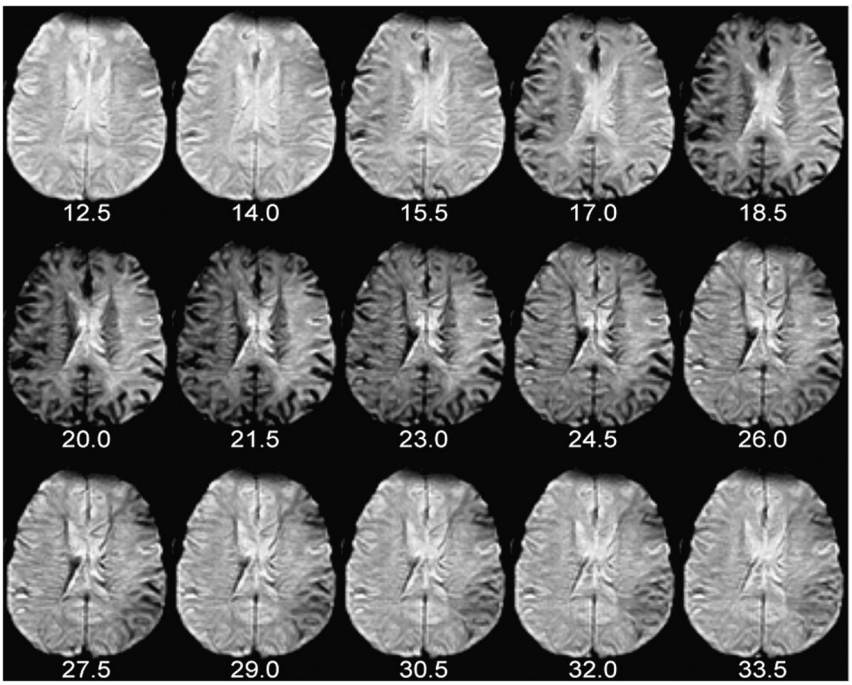

Figure 1. Dynamic susceptibility contrast (DSC) perfusion imaging

The number of seconds elapsed since the beginning of contrast injection appears beneath each image. Note the appearance of contrast in some large arteries, which become hypointense and "bloom" slightly, at 14.0 and 15.5 seconds post-injection (i.e. 24.0 and 25.5 seconds after the beginning of the scan). By 20.0 seconds post-injection, the presence of gadolinium in small vessels causes loss of parenchymal signal intensity in the normally perfused right hemisphere. Arrival of contrast is delayed and prolonged in the left hemisphere. These perfusion source images were used to create the graph and CBV maps in Figures 8 and 9, respectively.

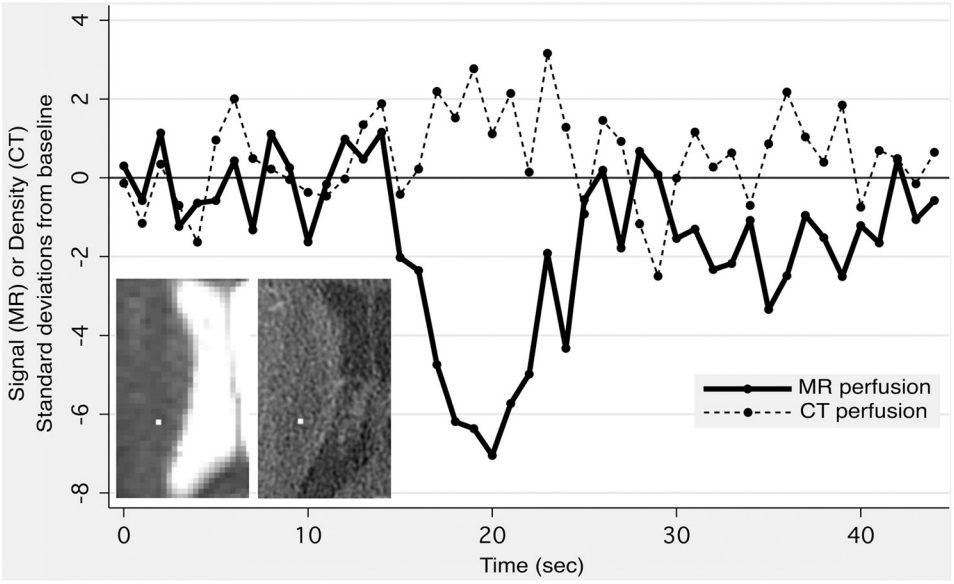

Figure 2. Comparison of MR and CT perfusion imaging

A 59-year-old male presented with slurred speech. DWI and CT angiography were normal, and the patient was subsequently diagnosed with ethanol intoxication. MR perfusion imaging (MRP) was performed 17 minutes after CT perfusion imaging (CTP). Identically sized regions of interest were placed on MRP (left inset, 1×1 pixel) and CTP (right inset, 4×4 pixels) source images in a randomly-selected location in the right corona radiata. The graph shows MR signal intensity and CT density as a function of time, with both expressed in terms of standard deviations above or below the mean value obtained from baseline images acquired before the arrival of the contrast bolus. Note the much larger signal change observed with MRP, compared to the changes observed with CTP, which are barely discernable from random noise fluctuations.

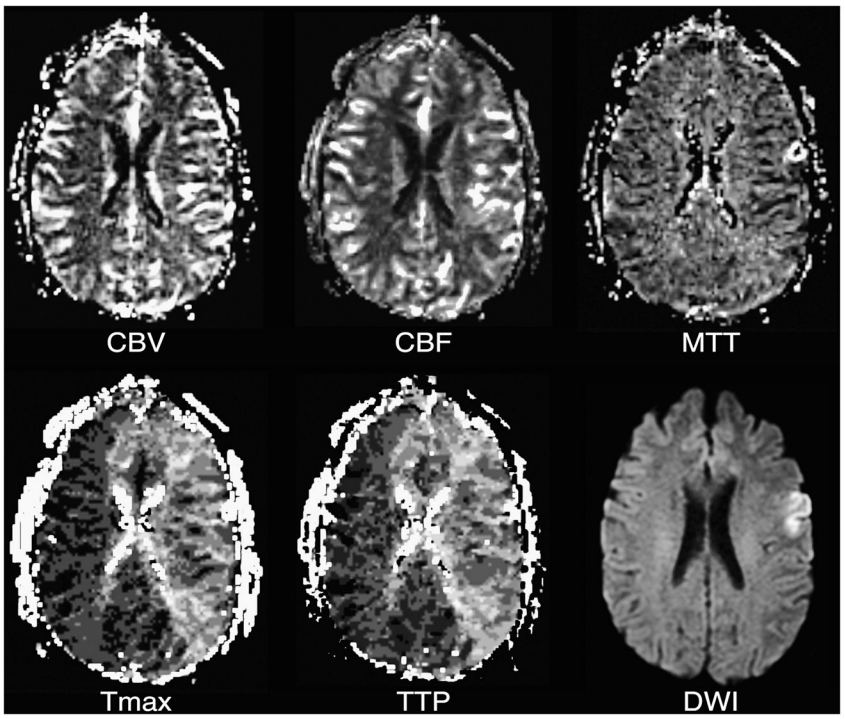

Figure 3. Delayed bolus arrival with preserved CPP

Tmax and TTP maps reflect delayed bolus arrival in most of the left cerebral hemisphere. Although there is the suggestion of slightly elevated CBF in some of the involved tissue, which could represent post-ischemic hyperperfusion, CBV, CBF, and MTT otherwise appear normal. A corresponding DWI image is presented for reference.

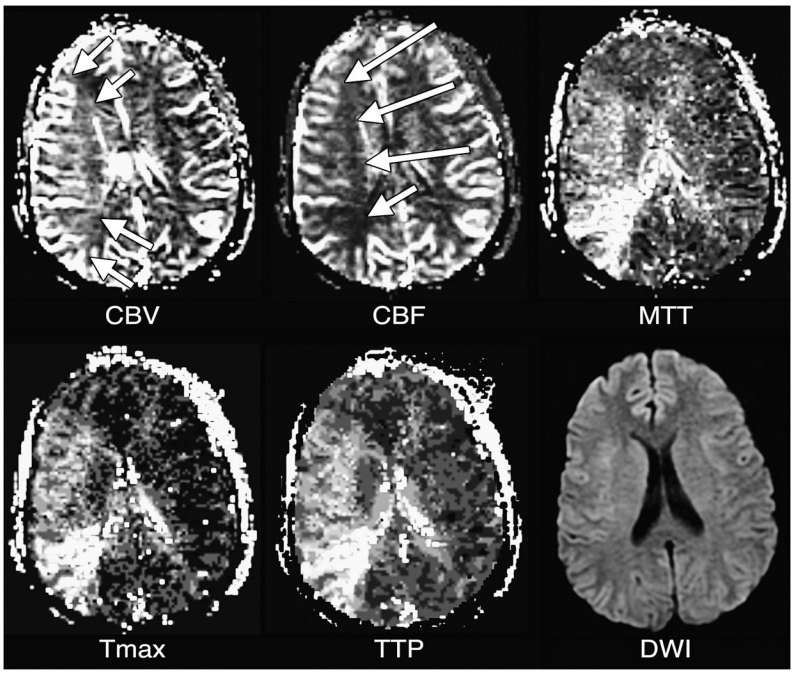

Figure 4. Compensated low CPP

Elevated CBV (arrows) in the right middle cerebral artery territory reflects vasodilation in response to decreased CPP. The CBF map shows that this response has been successfully in maintaining apparently normal CBF (arrows). MTT is elevated in the affected tissue. The Tmax map shows delayed bolus arrival. TTP is prolonged, probably as a result of both delayed bolus arrival and increased MTT. A corresponding DWI image is presented for reference.

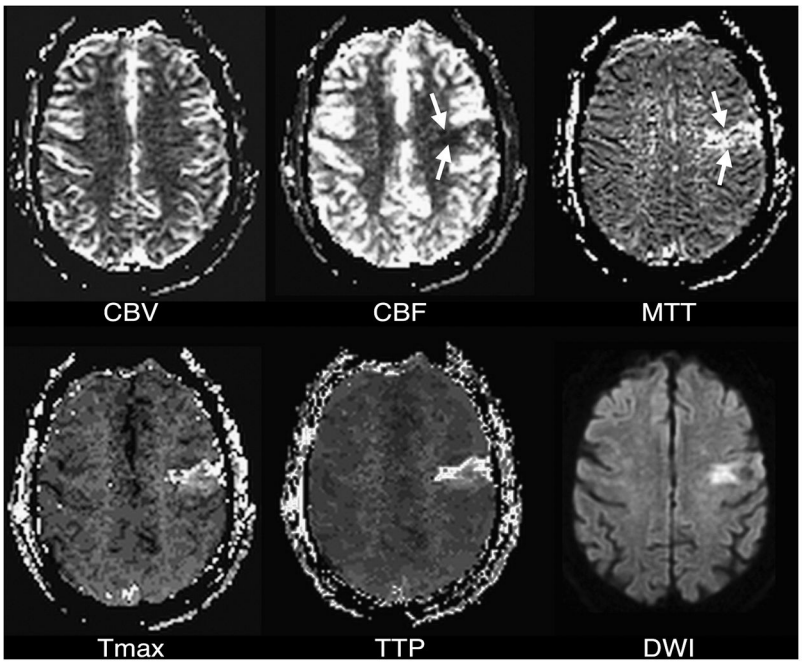

Figure 5. Hypoperfusion

CBF is decreased within a small wedge-shaped region in the left middle cerebral artery territory (arrows). There is a corresponding region of MTT prolongation (arrows). Tmax and TTP maps, as well as a DWI image, also show corresponding abnormalities.

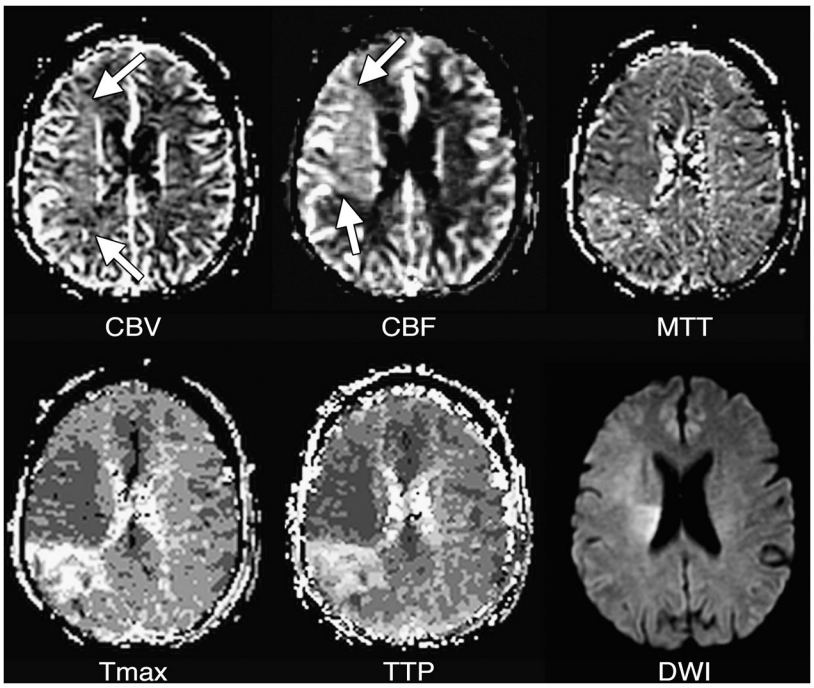

Figure 6. Post-ischemic hyperperfusion

CBV is slightly elevated (arrows) in most of the right middle cerebral artery territory, reflecting vasodilation. In most of this tissue, CBF is higher than normal (arrows), demonstrating the vasodilation has persisted following an ischemic insult. MTT in this tissue may be minimally decreased in the hyperperfused tissue, although normal or elevated MTT are sometimes seen in such conditions. The Tmax map shows that bolus arrival is early in the hyperperfused tissue, although normal or (rarely) delayed arrival also can be seen in post-ischemic hyperperfusion. Post-ischemic hyperperfusion can occur in tissue that did or did not experience irreversible injury, as shown by the DWI image, in which some but not all of the hyperperfused tissue appears abnormal. Note that there is a persistently underperfused region posterior to the hyperperfused area.

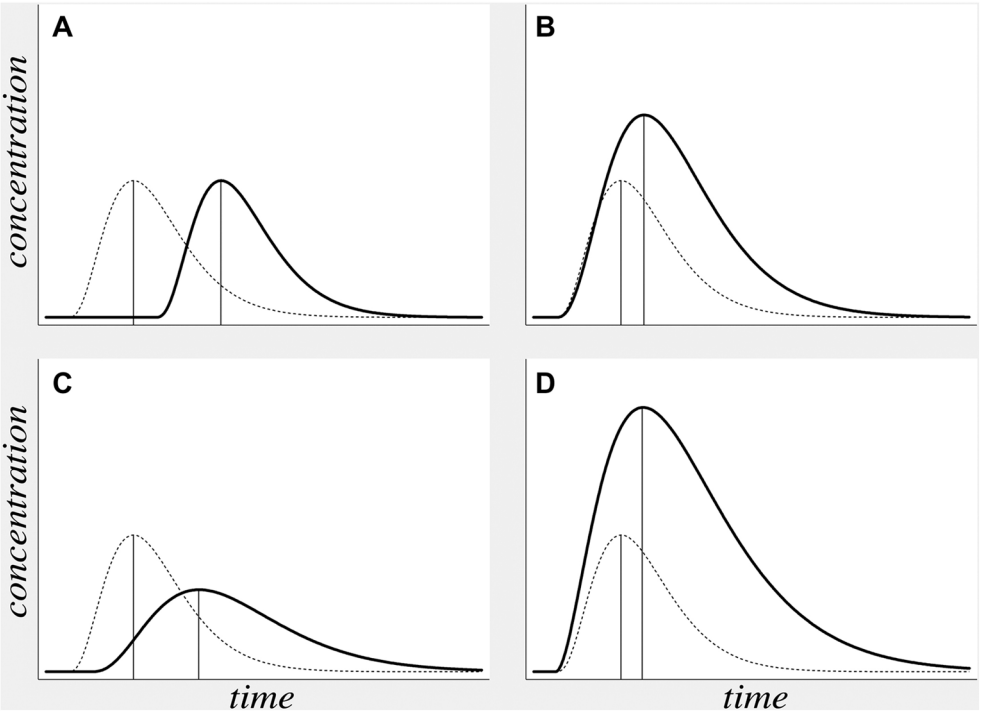

Figure 7. TTP delay in varying hemodynamic conditions

Theoretical concentration-versus-time curves (solid lines) reflect the four different abnormal hemodynamic conditions listed in Table 1: (A) delayed bolus arrival with preserved CPP, (B) compensated low CPP, (C) hypoperfusion, and (D) post-ischemic hyperperfusion. In each case, a concentration-versus-time curve for normal tissue is presented for comparison (dotted lines). TTP (vertical lines) can be delayed (i.e farther to the right) in all four conditions.

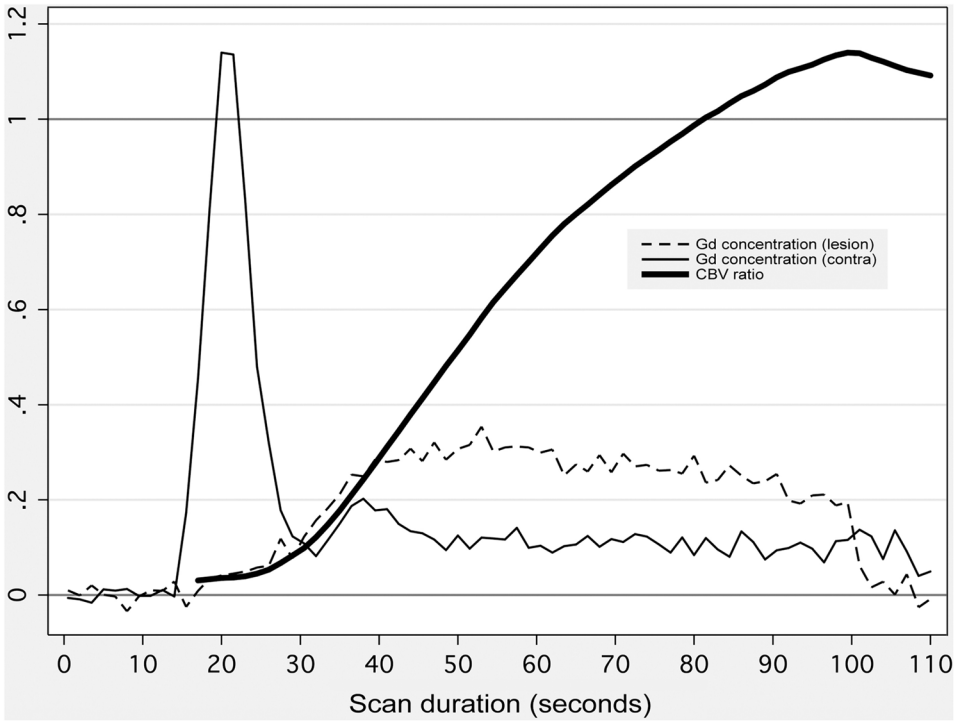

Figure 8. Effect of perfusion scan duration on calculated CBV

Thin lines depict gadolinium concentration (in arbitrary units) versus time following contrast injection, within small regions of interest (ROIs) placed in an acute stroke patient's low-CBF lesion (thin dashed line), and in the corresponding location in the unaffected contralateral hemisphere (thin solid line). ROI locations are show in Figure 9. Because of low blood flow, the curve rises much more slowly in the low-CBF lesion. CBV in each ROI (not shown) is calculated as the area under the concentration-versus-time curve. Therefore, for simulated short scan durations, the ratio of CBV in the lesion to normal CBV (thick solid line) is far below unity. However, when longer, more accurate scan durations are used, the ratio rises above unity, showing that CBV is actually elevated in the low-CBF ROI.

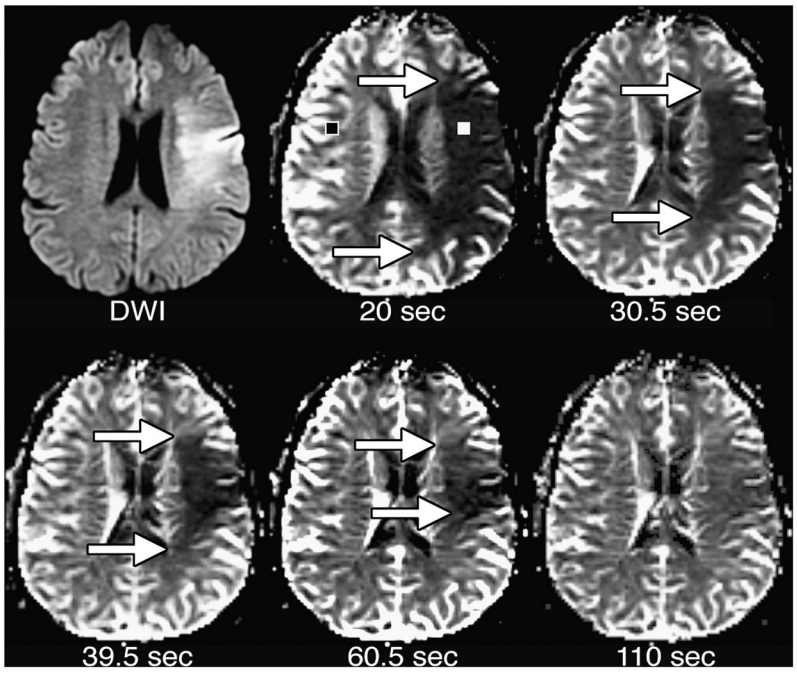

Figure 9. Effect of perfusion scan duration on CBV maps

CBV maps were made from the perfusion data shown in Figures 1 and 8. Maps were made using the entire scan, which lasted 110 seconds after contrast injection, as well as truncated data sets simulating the effects of shorter scan durations lasting 20, 30.5, 39.5, and 60.5 seconds after contrast injection. With the shortest scan duration of 20 seconds, there is a region of very low apparent CBV, which is much larger than the DWI lesion. With progressively longer scan durations, the size of the apparent CBV lesion shrinks. With the full 110-second scan duration, there is only a poorly delineated region of slightly reduced CBV that is considerably smaller than the DWI lesion.

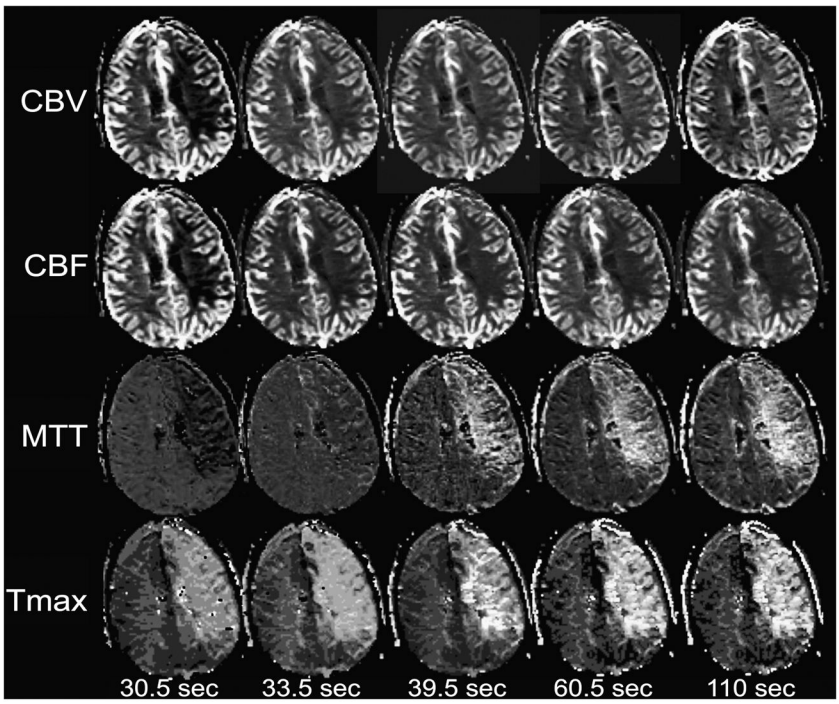

Figure 10. Effects of scan duration on various perfusion maps

Perfusion maps were made from a patient other than those depicted in previous figures, using data from the entire scan lasting 110 seconds after contrast injection, as well as temporally truncated subsets of the data simulating shorter scan durations. With the shortest scan duration of 30.5 seconds, there is a large low-CBV lesion occupying most of the left cerebral hemisphere. The apparent severity of CBV reduction is decreased with the 33.5-second scan, and no CBV lesion is apparent with the 39.5-second scan. With the 60.5- and 110-second scans, it is apparent that CBV is mildly elevated in the left hemisphere. CBF is artifactually reduced with the 30.5-second scan, but does not change significantly in the longer scans. Because MTT is calculated as the quotient of CBV divided by CBF, the effect of scan duration on CBV results in apparently reduced MTT with the shortest scan duration, and no obvious MTT lesion at 33.5 seconds, although a large region of prolonged MTT is clearly evident with longer scan durations. Tmax is not significantly changed by scan duration. DWI (not shown) was normal in this part of the brain.

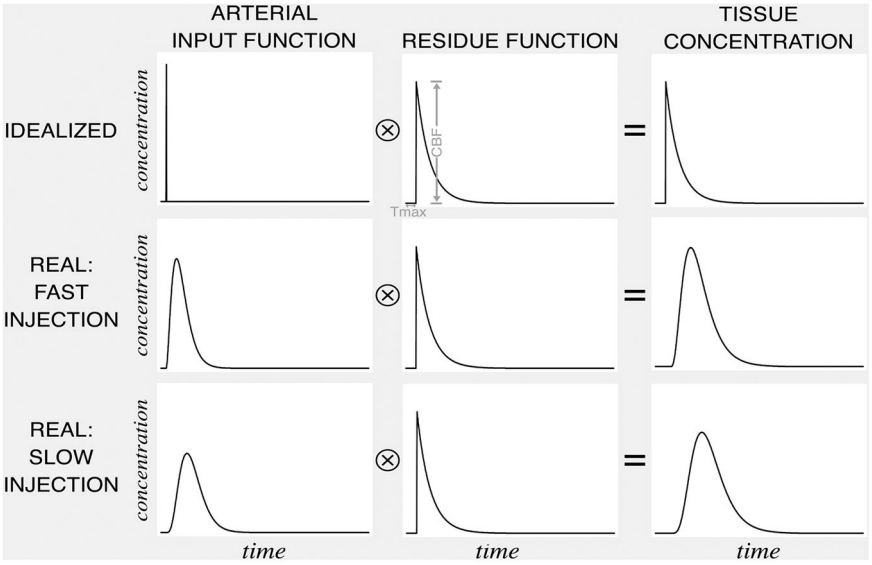

Figure 11. CBF, Tmax and convolution

Each voxel has a "residue function" reflecting the proportion of an idealized, instantaneously injected unit-sized contrast bolus that remains in the voxel following its arrival. The tissue concentration function is the convolution of the arterial input function (which varies depending on complex variables such as contrast bolus injection rate, cardiac output, and patient anatomy), and a multiple of the residue function that has been scaled by the value of CBF. The amplitude of this scaled residue function is CBF, and the time at which it reaches its maximum is Tmax. The scaled residue function cannot be observed directly. If both the concentration function and an arterial input function are known, the scaled residue function can be calculated by deconvolution.

Table 1

Distinguishing abnormal perfusion states using perfusion imaging.

	CBV	CBF	MTT	Timing parameters (e.g. Tmax)
Delayed arrival, preserved CPP	—	—	—	↑
Compensated low CPP	↑	—	↑	↑
Underperfused	↑↓	↓	↑↓	↑
Post-ischemic hyperperfusion	↑	↑	↑↓	↑↓ (usually ↓)

Table 2

Sample imaging parameters for MR perfusion imaging.

Pulse sequence: Gradient echo echo planar
Orientation: axial
Phase encoding direction: anterior-posterior
TR/TE/Flip angle: 1500 msec/40 msec/60 degrees
Field of view: 22 cm
Matrix size: 128 × 128
Slice thickness/interslice gap: 5 mm/1 mm
Number of slices: as many as permitted by scanner at TR≤1500 msec (approximately 14)
Number of acquisitions: 80
Pulse sequence duration: Two minutes
Contrast material: Gadopentatate dimeglumine, 20 cc, injected intravenously at 5 cc/s, beginning 10 seconds after initiation of the scan. Following the contrast agent injection, 20 cc of normal saline is injected at the same rate.